Title

Cooperative KaiA–KaiB–KaiC Interactions Affect KaiB/SasA Competition in the Circadian Clock of Cyanobacteria

Journal

Journal of Molecular Biology, 426(2)

ISSN

0022-2836

Authors

Tseng, Roger
Chang, Yong-Gang
Bravo, Ian
et al.

Publication Date

2014

DOI

10.1016/j.jmb.2013.09.040

Peer reviewed

Cooperative KaiA–KaiB–KaiC Interactions Affect KaiB/SasA Competition in the Circadian Clock of Cyanobacteria

Roger Tseng [1,2], Yong-Gang Chang [1], Ian Bravo [1], Robert Latham [1], Abdullah Chaudhary [3], Nai-Wei Kuo [1] and Andy LiWang [1,2,4,5]

*1 - **School of Natural Sciences,** University of California, Merced, CA 95343, USA*
*2 - **Quantitative and Systems Biology Graduate Group,** University of California, Merced, CA 95343, USA*
*3 - **School of Engineering,** University of California, Merced, CA 95343, USA*
*4 - **Chemistry and Chemical Biology,** University of California, Merced, CA 95343, USA*
*5 - **Center for Chronobiology,** Division of Biological Sciences, University of California, San Diego, La Jolla, CA 92093, USA*

***Correspondence to Andy LiWang:** 5200 North Lake Road, Merced, CA 95340, USA. Telephone: (209) 777-6341.*
aliwang@ucmerced.edu
http://dx.doi.org/10.1016/j.jmb.2013.09.040
Edited by A. G. Palmer III

Abstract

The circadian oscillator of cyanobacteria is composed of only three proteins, KaiA, KaiB, and KaiC. Together, they generate an autonomous ~24-h biochemical rhythm of phosphorylation of KaiC. KaiA stimulates KaiC phosphorylation by binding to the so-called A-loops of KaiC, whereas KaiB sequesters KaiA in a KaiABC complex far away from the A-loops, thereby inducing KaiC dephosphorylation. The switch from KaiC phosphorylation to dephosphorylation is initiated by the formation of the KaiB–KaiC complex, which occurs upon phosphorylation of the S431 residues of KaiC. We show here that formation of the KaiB–KaiC complex is promoted by KaiA, suggesting cooperativity in the initiation of the dephosphorylation complex. In the KaiA–KaiB interaction, one monomeric subunit of KaiB likely binds to one face of a KaiA dimer, leaving the other face unoccupied. We also show that the A-loops of KaiC exist in a dynamic equilibrium between KaiA-accessible exposed and KaiA-inaccessible buried positions. Phosphorylation at the S431 residues of KaiC shift the A-loops toward the buried position, thereby weakening the KaiA–KaiC interaction, which is expected to be an additional mechanism promoting formation of the KaiABC complex. We also show that KaiB and the clock-output protein SasA compete for overlapping binding sites, which include the B-loops on the CI ring of KaiC. KaiA strongly shifts the competition in KaiB's favor. Thus, in addition to stimulating KaiC phosphorylation, it is likely that KaiA plays roles in switching KaiC from phosphorylation to dephosphorylation, as well as regulating clock output.

Introduction

Evolution of life under daily swings of ambient light and temperature produced timekeeping systems called circadian clocks [1]. These cellular clocks prepare organisms for environmental oscillations by imposing circadian rhythms on gene expression, metabolism, physiology, and behavior in-phase with the rising and setting of the sun. These internal rhythms originate from the oscillator components of circadian clocks and are transmitted downstream through output pathways, resulting in clock control over cellular processes with important consequences to health and reproductive fitness [2–7]. At the other end, environmental cues entrain the oscillators through sensory input pathways. However, the mechanisms of biological timekeeping at the molecular level remain largely unresolved.

With regard to elucidating the molecular mechanics of circadian oscillators, most of the inroads have been made in the cyanobacterial system, which is composed of only three proteins, KaiA, KaiB, and KaiC [8] (Fig. 1). A mixture of these proteins from *Synechococcus elongatus* with ATP produces an autonomous, entrainable, and temperature-compensated circadian rhythm of KaiC autophosphorylation

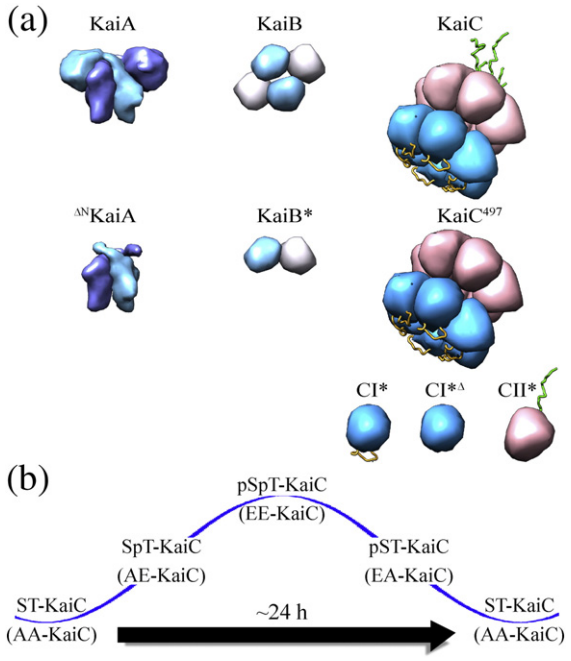

Fig. 1. A summary of KaiABC oscillator proteins and their variants used in this study.(a) Pictorial representations of wild-type cyanobacterial clock proteins: KaiA, KaiB, and KaiC as, respectively, homodimer, homotetramer, and homohexamer. Important variants of KaiA and KaiB and KaiC proteins used in this study are shown as well: $^{\Delta N}$KaiA (missing its N-terminal domain by truncating before residue S147), KaiB* (a dimeric variant by truncating after residue Y94 and with Y8A and Y94A substitutions) [24], KaiC^{497} (missing A-loops by truncating after I497) [18], CI* (monomeric CI domain: KaiC residues 1–247, with R41A and K173A substitutions) [24], CI*$^{\Delta}$ (same as CI*, but with the deletion of B-loop from residues 116–123), and CII* (monomeric CII domain: KaiC residues 249–518, with S431E, T432E, and E444D substitutions). Complete construct information is provided in Table S1.(b) A phosphorylation cycle of KaiC. ST-KaiC (unphosphorylated), SpT-KaiC (T432 phosphorylated), pSpT-KaiC (S431 and T432 phosphorylated), and pST-KaiC (S431 phosphorylated) can be mimicked by, respectively, AA-KaiC, AE-KaiC, EE-KaiC, and EA-KaiC. Alanyl/glutamyl substitutions mimic the unphosphorylated/phosphorylated states of S431 and T432.

and autodephosphorylation [9–11]. Recently, circadian rhythms of KaiC phosphorylation were also reconstituted *in vitro* using *Thermosynechococcus elongatus* proteins [12]. KaiC is a homohexamer in which each subunit is composed of two RecA-like domains, called CI and CII [13,14]. The CI and CII domains self-associate into rings and stack together similar to two donuts [15,16]. KaiA stimulates phosphorylation [17] by binding to the so-called A-loops of KaiC [18–20]. The A-loops are located at the pore of the CII ring. Each CII domain contains two residues, S431 and T432, which in the presence of KaiA phosphorylate (S → pS and T → pT) in the following order: ST → SpT → pSpT [21,22]. Upon phosphorylation of S431, the CII ring transitions from loose to tight and then stacks on the CI ring [23]. This stacking interaction exposes part of the KaiB binding site on CI [24]. KaiB binds to KaiC and inactivates KaiA [21,22]. KaiC then passes sequentially through the phosphoforms pSpT → pST → ST, whereupon the rings unstack and a new cycle begins. This ring–ring communication explained how phosphorylation on the CII ring could induce new protein–protein interactions on the CI ring. Recently, it was demonstrated that dephosphorylation likely proceeds through phosphoryl transfer from KaiC to bound ADP molecules, followed by hydrolysis of the newly formed ATP intermediates [25,26].

With regard to entrainment, instead of having photoreceptor-mediated input pathways, the cyanobacterial clock relies on metabolic products of photosynthesis [27,28]. Oxidized quinones signal the onset of darkness by directly binding to and inactivating KaiA [29,30] and the input pathway protein CikA [31–34], whereas high ADP/ATP ratios, which act directly on KaiC, are a measure of the duration of darkness [35]. Through output pathways, the cyanobacterial clock controls cellular processes such as genome-wide gene expression [36–39] and cell division [40,41]. The output pathway protein SasA [42], a sensor histidine kinase, receives timing signals from the oscillator through direct interactions of its N-terminal domain with KaiC. This interaction stimulates SasA phosphorylation [43] and subsequent phosphoryl transfer to and activation of the transcription factor RpaA [44]. Whereas SasA can bind to each phosphoform of KaiC [45], KaiB only binds to KaiC when the S431 residues are phosphorylated [21,22], and it can displace SasA from those phosphoforms [12,46]. Interestingly, stimulation of CikA by the KaiB–KaiC complex during the subjective night induces dephosphorylation of RpaA [47]. Thus, rhythms in KaiB–KaiC binding may regulate clock output by controlling sequential and reciprocal action of SasA and CikA on RpaA. Recently, we showed that both SasA [23] and KaiB [24] bind to the CI domain of KaiC, suggesting that they compete for overlapping binding sites.

Until now, it has been thought that KaiA only stimulates KaiC phosphorylation [17,48] and signals the onset of darkness [27]. In other words, KaiA has not been presumed to play active roles in the dephosphorylation of KaiC or clock output. Here, using proteins from *T. elongatus*, we investigated whether those two presumptions are warranted. We show that, in fact, KaiA plays a cooperative role in the assembly of the KaiA–KaiB–KaiC dephosphorylation complex and that decreasing KaiA–KaiC affinities during KaiC phosphorylation enhances this cooperativity. We also show that KaiA promotes the displacement of SasA

by KaiB from KaiC, implicating KaiA as one of the regulators of clock output. Apparently, a dimer of KaiA binds only one KaiB monomer. Additionally, we show that KaiB and SasA bind to the B-loop of the CI domain of KaiC.

Results

Resolving whether the N-terminal domains of KaiA are necessary for binding KaiB

The N-terminal domains of KaiA from *S. elongatus* have recently been demonstrated to play a critical role in entrainment by sensing oxidized quinones [27]. An X-ray crystal structure of KaiA verified that the N-terminal domains bind directly to the oxidized form of quinone analog 2,5-dibromo-3-methyl-6-isopropyl-*p*-benzoquinone [30]. Less clear is the role of the N-terminal domains in generating KaiC phosphorylation rhythms. Recent electron microscopy (EM) studies have suggested that, in order for KaiC to dephosphorylate, KaiB sequesters monomeric subunits of KaiA by binding exclusively to its N-terminal domains [46]. If correct, the N-terminal domains of KaiA would be necessary for the generation of phosphorylation rhythms. However, electron spin resonance spectroscopy suggests that the C-terminal domains of KaiA bind KaiB [49]. Additionally, *Anabaena* sp. strain PCC-7120, which supposedly displays circadian rhythms [50], lacks N-terminal domains [51]. Also, truncating the N-terminal domains of KaiA did not abolish *in vivo* rhythms of bioluminescence [52]. We therefore wanted to clarify these contradicting models. In Fig. 1, we provided a list of the different constructs of KaiA, KaiB, and KaiC used in this study.

Here, using size-exclusion chromatography of *T. elongatus* proteins, we found that a KaiA construct, $^{\Delta N}$KaiA, which lacked its N-terminal domains by truncating before residue S147 (Fig. 1a), formed a stable ternary complex with KaiB* (a dimeric variant of KaiB) [24] and CI* (a monomeric variant of the CI domain) [24] (Fig. 2a, left panel). Because KaiB* binds to CI as a monomer [24], it is likely that KaiB* is a monomer in this ternary complex as well. Next, we tested formation of $^{\Delta N}$KaiA–KaiB*–CI* by NMR. Chemical shift perturbations in methyl-TROSY (*t*ransverse *r*elaxation *o*ptimized *s*pectroscop*y*) NMR [53] spectra of U-[^{15}N, ^{2}H]-Ile-δ1-[^{13}C, ^{1}H]$^{\Delta N}$KaiA in the presence of unlabeled KaiB* and CI* (Fig. 3a, columns 1 and 2) also indicated complex formation, corroborating our chromatography results.Identical spectra were obtained when using KaiB (wild type) instead of KaiB* to form the $^{\Delta N}$KaiA–KaiB–CI* complex (Fig. 3a, column 3), suggesting that these interactions are not artifacts from using a mutant of KaiB. As further evidence that the N-terminal domains of KaiA are not necessary for KaiA–KaiB interactions, a full phosphorylation cycle was observed using $^{\Delta N}$KaiA instead of KaiA (Fig. S3a and b). Thus, the recent model in which the N-terminal domains of KaiA are necessary for KaiA–KaiB binding [46], albeit in the *S. elongatus* system, may need to be revised. Previously, we showed that a construct of KaiA missing residues 1–179 could not be sequestered by KaiB [18], which together with the data here suggests that the linker connecting the N- and C-terminal domains, residues 147–179, plays a role in KaiA–KaiB interactions. $^{\Delta N}$KaiA was used for NMR experiments because of its smaller size and labeled for fluorescence experiments because it retains only one of four naturally occurring cysteinyl residues (C272) for convenient labeling with thiol-reactive fluorophores.

Assembly of the KaiA–KaiB–KaiC complex is a cooperative process

Even after several hours of incubation, there were no detectable interactions between $^{\Delta N}$KaiA and KaiB (Fig. 3a, column 4). However, CI* significantly enhanced $^{\Delta N}$KaiA–KaiB binding (Fig. 3a, column 3). Similarly, others have observed that KaiC enhances the otherwise weak interaction between KaiA and KaiB [11,13,54]. In contrast to KaiB, KaiB* bound to $^{\Delta N}$KaiA even in the absence of CI* (Fig. 2a, left panel; Fig. 3a, columns 5 and 6). Recall that the stable forms of free KaiB and KaiB* are homotetramer [55–57] and homodimer [24], respectively. Based on our findings, we propose that the dimer is closer to the conformation that binds KaiC and KaiA than the tetramer. This idea is supported by recent findings that KaiB* binds more rapidly to CI* than does KaiB [12,24].

As with KaiB, the weak $^{\Delta N}$KaiA–KaiB* interaction was significantly enhanced by CI*. Free $^{\Delta N}$KaiA or KaiB* was undetectable by gel-filtration chromatography in the presence of CI*, in contrast to when CI* was absent (Fig. 2a, left panel). Similarly, NMR spectra of labeled $^{\Delta N}$KaiA showed complete KaiB* binding in the presence of CI* (Fig. 3a, column 2) but incomplete binding without CI* (Fig. 3a, columns 5 and 6). The absence of an observable interaction between just $^{\Delta N}$KaiA and CI* (Fig. 3a, column 7; Fig. S1a) suggests that CI* facilitates KaiA–KaiB binding solely through interactions with KaiB. The observation that the majority of the NMR peaks of KaiB*-bound $^{\Delta N}$KaiA had the same chemical shifts in the presence and absence of CI* also supports this notion (Fig. 3a, columns 2 and 3 and columns 5 and 6). Although $^{\Delta N}$KaiA did not interact with CI*, NMR spectra showed, as expected, that $^{\Delta N}$KaiA interacted with CII*, a monomeric variant of the CII domain [18] (Fig. 3a, column 8). These observations support the model in which KaiA has two distinct binding sites, the A-loop during KaiC phosphorylation [18] and KaiB during dephosphorylation [24,54,58].

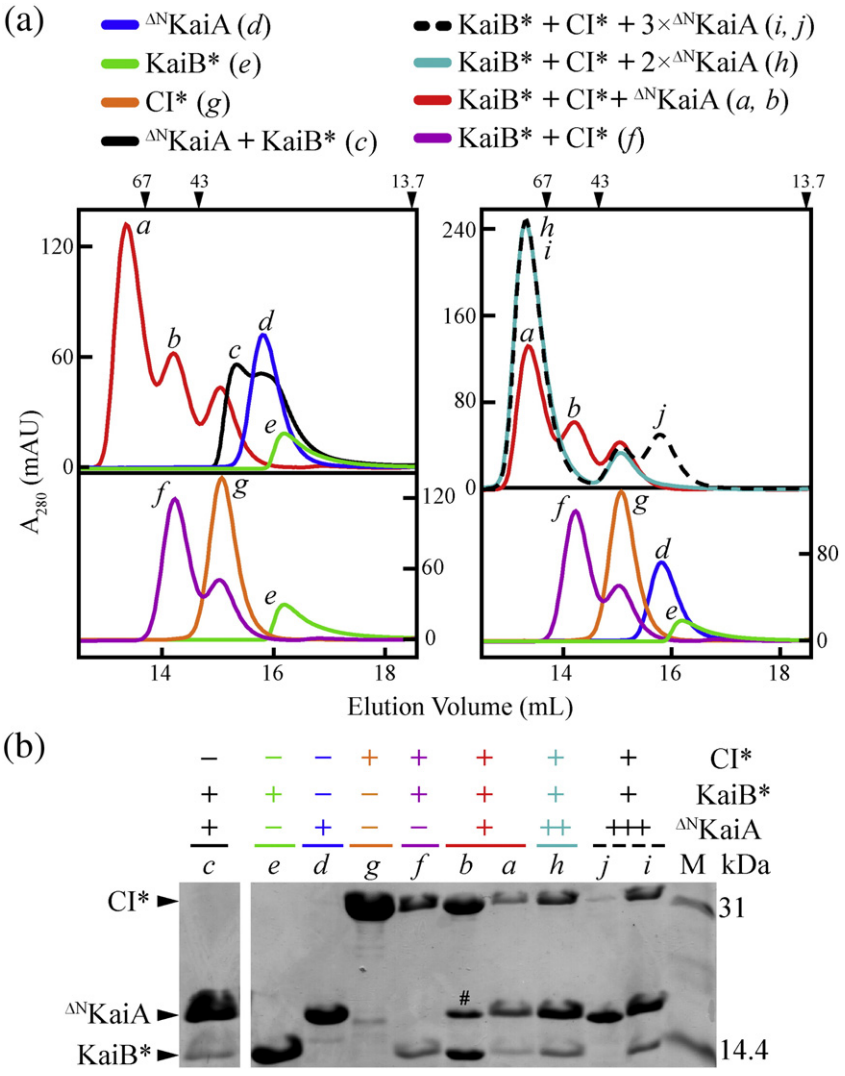

Fig. 2. Formation of $^{\Delta N}$KaiA–KaiB*–CI* and $^{\Delta N}$KaiA–KaiB* complexes.(a) Gel-filtration profiles of KaiB* + CI* + $^{\Delta N}$KaiA (red), $^{\Delta N}$KaiA + KaiB* (black), $^{\Delta N}$KaiA alone (blue), and KaiB* alone (green) (top left). Control mixtures of KaiB* + CI* (purple), CI* alone (orange), and KaiB* alone (green) are shown below for comparison (bottom left). Gel-filtration profiles of KaiB* + CI* + $^{\Delta N}$KaiA with increasing amounts of $^{\Delta N}$KaiA added are shown on the top right panel (1×, red; 2×, cyan; 3×, black dash). Control mixtures of KaiB* + CI* (purple), CI* alone (orange), $^{\Delta N}$KaiA alone (blue), and KaiB* alone (green) are shown below for comparison (bottom right). 1× corresponds to 50 μM monomer concentration. Chromatogram of $^{\Delta N}$KaiA + CI* is shown in Fig. S1a. Molecular mass markers in kilodaltons (kDa) are marked by black arrows along the top of the gel-filtration chromatograms. Peaks denoted by *a*, *b*, *c*, *d*, *e*, *f*, *g*, *h*, *i*, and *j* were checked by SDS/PAGE. For details on the protein constructs and experimental setup, please see Table S1.(b) SDS/PAGE gel of peaks *a*, *b*, *c*, *d*, *e*, *f*, *g*, *h*, *i*, and *j* in (a). All lanes shown were run on the same gel. The band marked "#" in lane *b* indicates the presence of $^{\Delta N}$KaiA in peak *b*. A comparison of peak *b* with peaks from other chromatograms (*f*, *h*, and *i*) suggests that the presence of $^{\Delta N}$KaiA in *b* was likely due to overlap of peaks *a* and *b* in the 1:1:1 $^{\Delta N}$KaiA:KaiB*:CI* chromatogram. The presence of a peak corresponding to free CI* in the 1:1:1, 2:1:1, and 3:1:1 $^{\Delta N}$KaiA:KaiB*:CI* chromatograms suggests that the true concentration of CI* was systematically underestimated. This underestimation however did not affect our analysis because CI* and $^{\Delta N}$KaiA do not interact with each other directly.

Now that we have demonstrated that CI* facilitates KaiA–KaiB binding, we tested the extent to which KaiA facilitates KaiB–KaiC binding. We measured the apparent dissociation constants, K_D^{app}, for the KaiB–CI* complex in the presence and absence of saturating amounts of KaiA (wild type), by monitoring the fluorescence anisotropy of labeled KaiB (Fig. 3b). Indeed, we found that KaiA decreased the K_D^{app} 10-fold, from 20.5 ± 1 μM to 2.0 ± 0.4 μM, indicating positive cooperativity (cooperativity factor of 0.10 ± 0.02). Thus, our results suggest that the switch from KaiC phosphorylation to dephosphorylation is

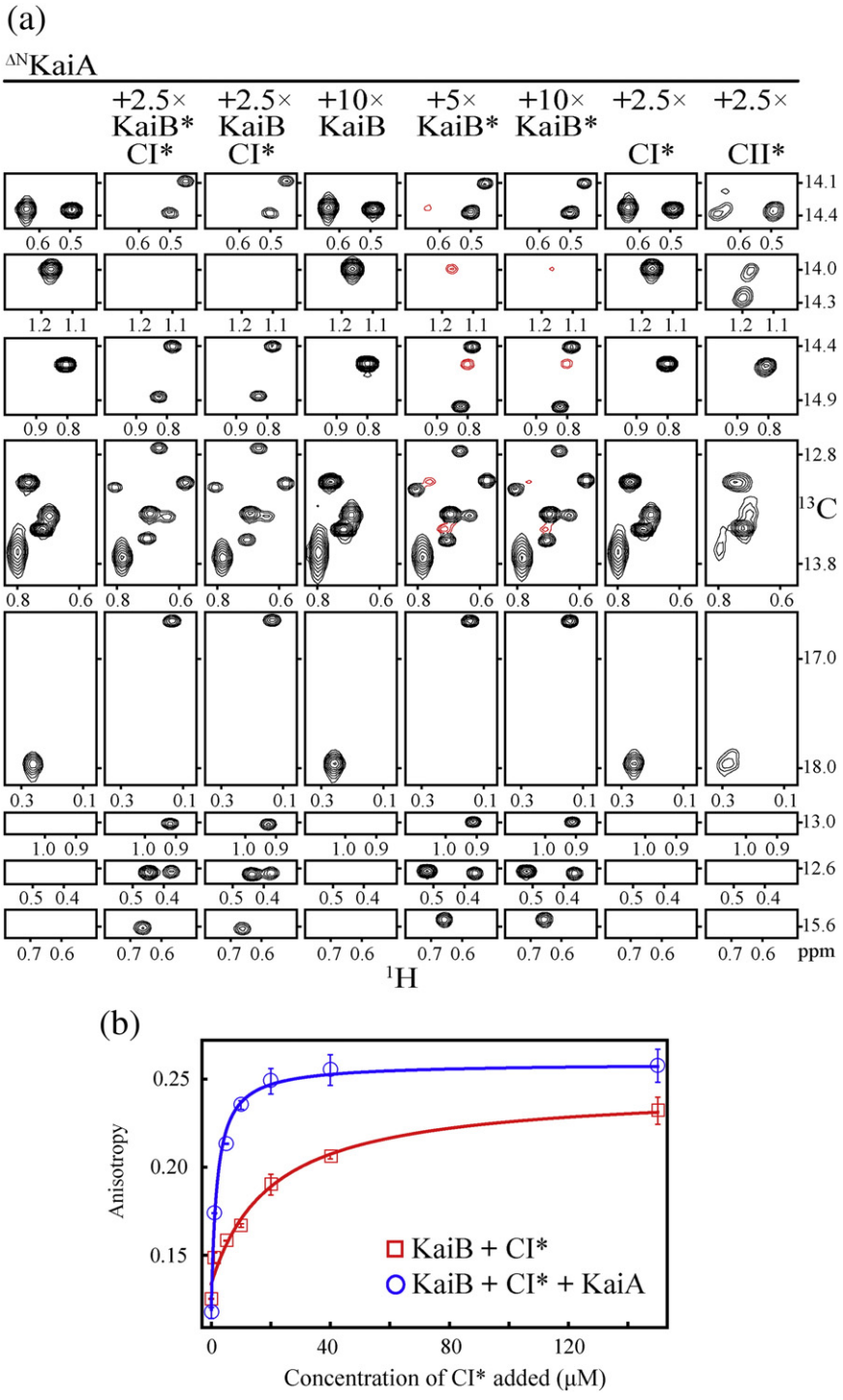

Fig. 3. Formation of a $^{\Delta N}$KaiA–KaiB*–CI* complex is a cooperative process.(a) Selected regions from methyl-TROSY spectra of 1× U-[^{15}N, ^{2}H]-Ile-δ1-[^{13}C, ^{1}H] $^{\Delta N}$KaiA alone (column 1) or in the presence of 2.5× (KaiB* + CI*) (column 2), 2.5× (KaiB + CI*) (column 3), 10× KaiB (column 4), 5× KaiB* (column 5), 10× KaiB* (column 6), 2.5× CI* (column 7), or 2.5× CII* (column 8). 1× corresponds to 20 μM monomer concentration. NMR peaks marked in red are at positions that correspond to resonances in free $^{\Delta N}$KaiA (columns 4 and 5). Full spectra are shown in Fig. S2. For details on the protein constructs and experimental setup, please see Table S1.(b) Fluorescence anisotropy data to measure apparent dissociation constants, K_D^{app}, of 6-IAF-labeled KaiB binding to CI* in the presence (blue) or absence (red) of 5 μM KaiA. Data were fit to equation (2) in Supplementary Material. The K_D^{app} values for CI* and CI* + KaiA are 20.5 ± 1.0 and 2.0 ±0.4 μM, respectively. Standard error was estimated from duplicate measurements. Equilibrium prior to measurements was achieved by incubation of samples for 24 h (Fig. S4a). For details on the protein constructs and experimental setup, please see Table S1.

promoted by cooperative formation of the KaiA–KaiB–KaiC complex.

Estimating the stoichiometry of the KaiA–KaiB complex

So far, the structural details of the KaiA–KaiB complex in the dephosphorylation phase of KaiC remain largely unclear. The stoichiometry of the KaiA–KaiB complex was recently estimated by gel-filtration chromatography to be a dimer of KaiB bound to a dimer of KaiA [49]. In a two-fold symmetric complex, each symmetry-related pair of spins would produce a single observable NMR signal. However, the number of peaks in methyl-TROSY spectra of U-[^{15}N, ^{2}H]-Ile-δ1-[^{13}C, ^{1}H]$^{\Delta N}$KaiA almost doubled upon binding KaiB*, not counting the peaks that corresponded to unbound $^{\Delta N}$KaiA (Fig. S2). In the spectrum of free $^{\Delta N}$KaiA, there were nine methyl peaks as was expected for a symmetric homodimer with nine isoleucine residues per subunit [59]. However, 16 new $^{\Delta N}$KaiA peaks appeared upon adding unlabeled KaiB*. These new peaks persisted after forcing all $^{\Delta N}$KaiA into the complex by adding CI* (Fig. 3a, column 1 and 2), indicating that the new peaks were from the bound form of $^{\Delta N}$KaiA. This 1.8-fold increase in the number of NMR peaks suggests that the symmetry of $^{\Delta N}$KaiA was broken by KaiB*. Although dramatic changes in the ^{15}N TROSY spectra of [^{15}N, ^{2}H]KaiB* upon binding unlabeled $^{\Delta N}$KaiA suggested that KaiB* changed its structure globally, the number of peaks remained similar (Fig. S5a). A model consistent with these observations is one in which KaiB binds as a monomer to one face of the $^{\Delta N}$KaiA dimer. This binding may distort the other face such that a second KaiB monomer cannot bind.

The idea of a monomeric subunit of KaiB binding to a KaiA dimer is also supported by size-exclusion chromatography (Fig. 2a, right panel). We ran mixtures of $^{\Delta N}$KaiA:KaiB*:CI* at monomer molar ratios of 1:1:1, 2:1:1, and 3:1:1. At 1:1:1, both KaiB*–CI and $^{\Delta N}$KaiA–KaiB*–CI complexes were observed. However, in the 2:1:1 mixture, the KaiB*–KaiC complex disappeared and, similar at 1:1:1, no free $^{\Delta N}$KaiA was detected. Only at the 3:1:1 ratio was free $^{\Delta N}$KaiA observed. Together, the data suggest that one subunit of KaiB binds one subunit of CI and two subunits of KaiA at the C-terminal and linker regions. The hydrophobic nature of the dimer interface of KaiA [60] makes it improbable that KaiA disassociates into monomeric subunits with that interface exposed [46].

Phosphoryl-S431 of KaiC imposes negative feedback on the KaiA–KaiC interaction

KaiA stimulates KaiC phosphorylation by binding to exposed A-loops [18,61]. Thus, dephosphorylation of KaiC requires sequestration of KaiA away from the A-loops in a KaiA–KaiB–KaiC complex. Interestingly, there seems to be a KaiB-independent negative feedback mechanism on KaiA–KaiC interactions that may facilitate sequestration. The affinity of KaiA for unphosphorylated KaiC is higher than that for phosphorylated KaiC [62,63]. A mathematical model has suggested that such negative feedback could play a role in maintaining phase coherence across an ensemble of Kai proteins [64]. The high-resolution structure of a complex between KaiA and its binding site on KaiC, which includes the A-loop residues (residues 487–497), suggested that regulation of the A-loops between a KaiA-accessible exposed position and a KaiA-inaccessible buried position (as found in the crystal structure [16]) is a possible mechanism for negative feedback [18]. However, since the A-loops have only been observed in their buried position, the idea of a dynamic equilibrium between buried and exposed positions needed to be tested. As such, A-loop exposure was gauged by the kinetics of their proteolysis, k_{obs}, at a thrombin cut site (LVPRGS) that replaced a naturally occurring stretch of residues, I497–K502, immediately following the A-loop. We reasoned that the accessibility of the proteolysis site would depend on the

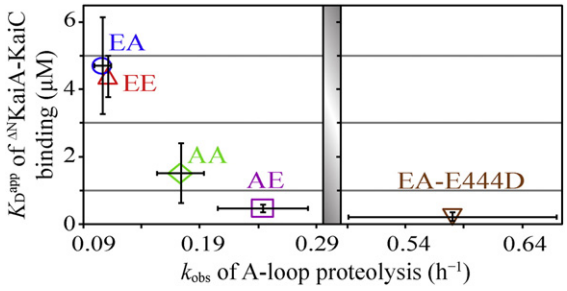

Fig. 4. A-loop exposure is correlated with KaiA–KaiC affinity. Kinetics of A-loop proteolysis of five variants of KaiC (AA-KaiC, green diamond; AE-KaiC, purple square; EE-KaiC, red triangle; EA-KaiC, blue circle; EA-KaiC^{E444D}, brown inverted triangle) with a thrombin cut site (LVPRGS) replacing residues I497 to K502. A-loop proteolysis rates were determined by fitting time points resolved by SDS/PAGE (Fig. S6a and b) to equation (5) in Supplementary Material. k_{obs} (h^{-1}) for AA-, AE-, EE-, EA-, and EA-E444D are 0.17 ± 0.02, 0.24 ± 0.04, 0.111 ± 0.001, 0.106 ± 0.007, and 0.58 ±0.09, respectively. $^{\Delta N}$KaiA–KaiC affinity, K_D^{app}, was determined from the dependence of fluorescence anisotropy of 6-IAF labeled $^{\Delta N}$KaiA on the concentration of the same five phosphomimic variants of KaiC, but without the thrombin cut sites. The K_D^{app} values, obtained from fitting the data to equation (1) in the Supplementary Material, for AA-, AE-, EE-, EA-, and EA-E444D are 1.5 ± 0.9, 0.5 ± 0.1, 4.4 ± 0.6, 4.7 ± 1.4, and 0.2 ± 0.1 μM, respectively (Fig. S6c). Standard errors for k_{obs} and K_D^{app} were estimated from duplicate measurements as shown in Fig. S6. For details on the protein constructs and experimental setup, please see Table S1.

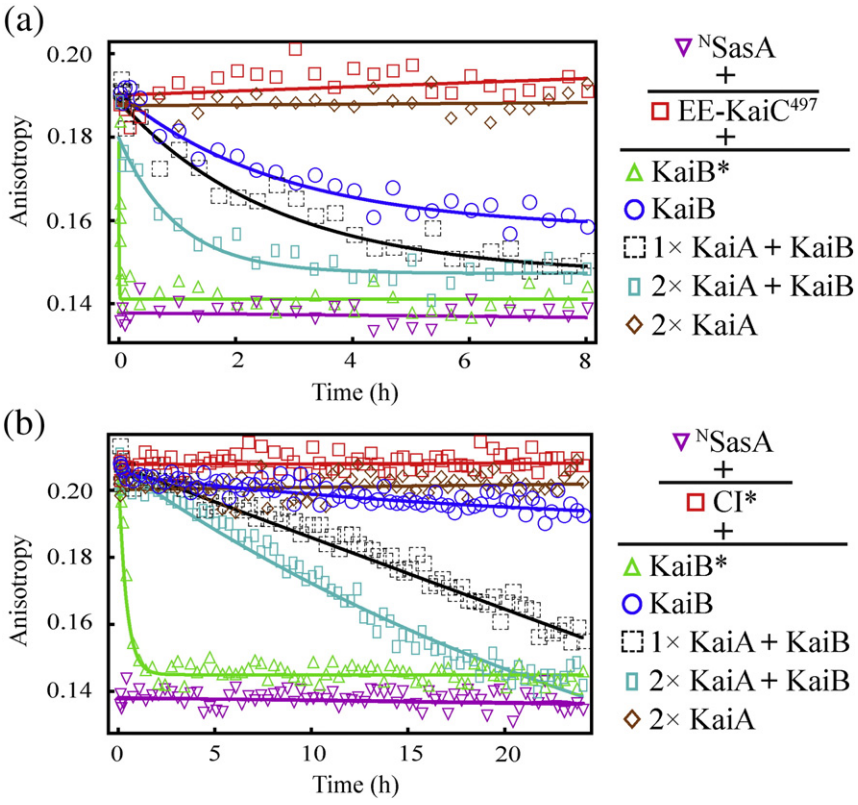

Fig. 5. KaiA as a modulator of KaiB/SasA competition for KaiC and CI.(a) Fluorescence anisotropy of competition kinetics of 6-IAF-labeled ^{N}SasA alone (purple), ^{N}SasA + EE-KaiC^{497} (red), ^{N}SasA + EE-KaiC^{497} + KaiB* (green), ^{N}SasA + EE-KaiC^{497} + KaiB (blue), ^{N}SasA + EE-KaiC^{497} + KaiB + 1× KaiA (black), ^{N}SasA + EE-KaiC^{497} + KaiB + 2× KaiA (cyan), and ^{N}SasA + EE-KaiC^{497} + 2× KaiA (brown). 1× corresponds to 10 μM monomer concentration. For details on the protein constructs and experimental setup, please see Table S1. Details on fitting the data to a single exponential equation are provided in the Supplementary Material.(b) Fluorescence anisotropy of competition kinetics of 6-IAF-labeled ^{N}SasA alone (purple), ^{N}SasA + CI* (red), ^{N}SasA + CI* + KaiB* (green), ^{N}SasA + CI* + KaiB (blue), ^{N}SasA + CI* + KaiB + 1× KaiA (black), ^{N}SasA + CI* + KaiB + 2× KaiA (cyan), and ^{N}SasA + CI* + 2× KaiA (brown). 1× corresponds to 10 μM monomer concentration. For details on the protein constructs and experimental setup, please see Table S1. Differences in the kinetics between (a) and (b) suggest that the hexameric EE-KaiC^{497} and monomeric CI* do not interact identically with ^{N}SasA and KaiB.

dynamic equilibrium of the A-loops between buried and exposed positions. We inserted the thrombin cut site in XY-KaiC variants where X and Y, at positions 431 and 432, respectively, were substituted with alanyl/glutamyl residues to mimic the unphosphorylated/phosphorylated states of S431 and T432 of KaiC. Thus, AA-, AE-, EE-, and EA-KaiC variants mimic, respectively, ST-KaiC (unphosphorylated), SpT-KaiC (only T432 phosphorylated), pSpT-KaiC (both residues phosphorylated), and pST-KaiC (only S431 phosphorylated) (Fig. 1b). Several studies have shown that these KaiC mutants are reasonably faithful mimics of the naturally occurring phosphoforms [40,65,66]. Each of the four phosphomimics of KaiC containing the thrombin cut site was incubated with the protease under identical conditions. Time points were analyzed by SDS/PAGE. EA- and EE-KaiC had slower rates of proteolysis, that is, smaller values of k_{obs}, than AA- and AE-KaiC (Fig. 4 and Fig. S6a and b), suggesting that the A-loops made fewer excursions from the buried to the exposed position in the pST- and pSpT-KaiC phosphomimics. Thus, phosphorylation at S431, which tightens the CII ring [23], likely shifts the A-loop equilibrium toward the buried position, where the A-loops can form a ring of hydrogen-bonding interactions that cooperate with phosphoryl-S431 to tighten the CII ring [18].

Because an A-loop comprises one-third of the KaiA binding site [18,20] (the other two-thirds being the C-terminal tail of the CII domain of KaiC), promoting A-loop burial is predicted to weaken KaiA–KaiC binding. Thus, we also measured apparent K_D values, K_D^{app}, of the KaiA–KaiC interaction, as a function of concentration of KaiC phosphomimics, using fluorescence anisotropy of labeled $^{\Delta N}$KaiA proteins (Fig. 4 and Fig. S6c). As shown in Fig. 4, the

affinity decreases ~10-fold from AE-KaiC to EA-KaiC. Although this change is modest, it should be noted that similarly modest changes were sufficient to reproduce KaiC phosphorylation rhythms *in silico* [63]. In Fig. 4, a trend was observed with smaller k_{obs} correlating with larger K_D^{app}, suggesting that the KaiA-stimulated phosphorylation of S431 imposes negative feedback by

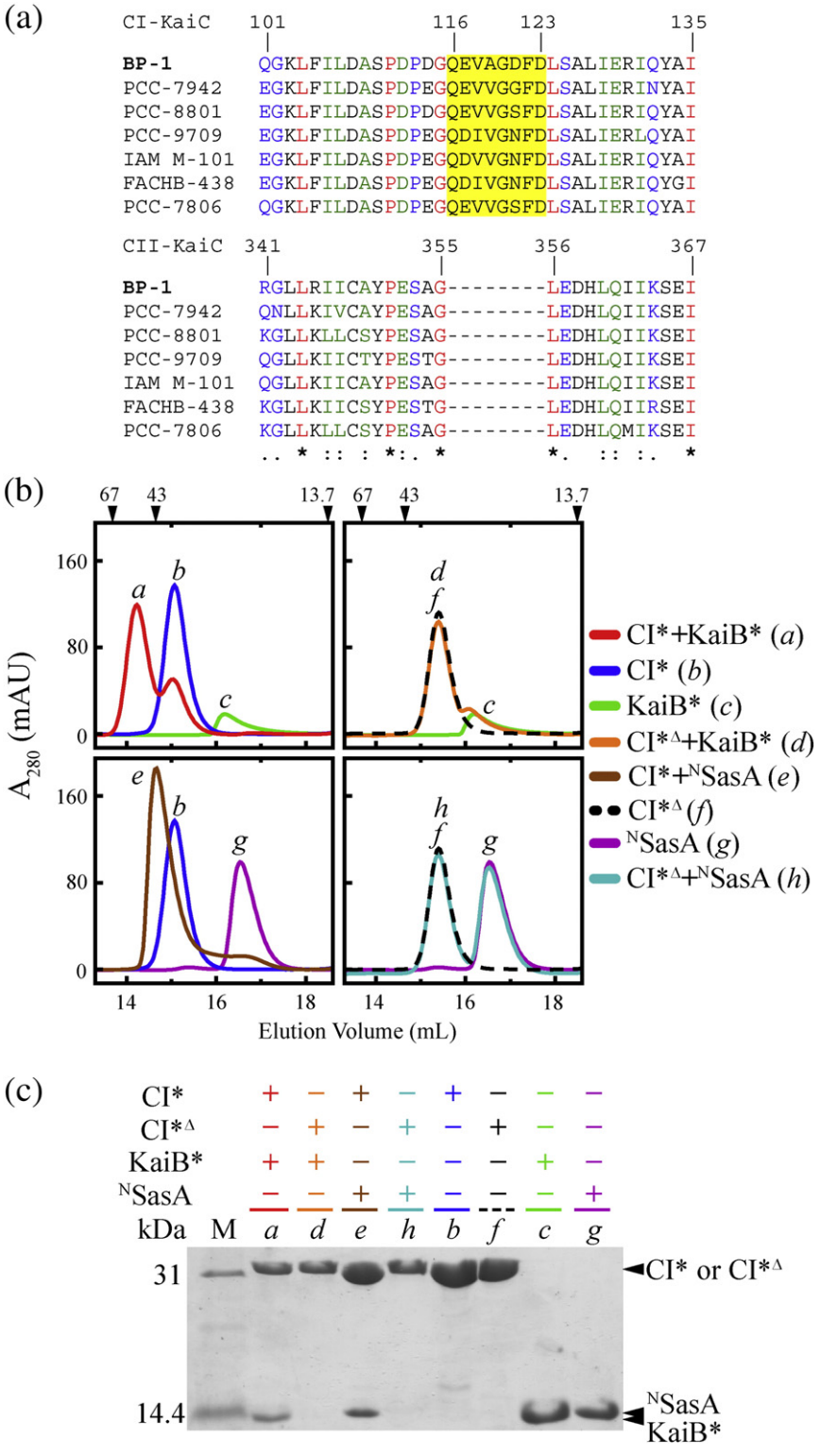

promoting burial of part of the KaiA binding site on KaiC. Using just two phosphomimics (AA-KaiC and EE-KaiC), Qin *et al.* reported an opposite trend in KaiA–KaiC affinities using *S. elongatus* proteins [54]. Thus, it was important that we validated our results. Residue E444 of KaiC appears to stabilize the buried form of the A-loops through side-chain hydrogen bonds. Because destabilizing the buried position of the A-loops activates the autokinase activity of KaiC [18], we could gauge the affect of the E444D substitution on the A-loops by its affect on KaiC phosphorylation. In fact, the E444D substitution produced constitutively hyperphosphorylated mutants in both *S. elongatus* [18] and *T. elongatus* KaiC proteins (Fig. S3c and d). To verify whether E444D indeed acted by destabilizing the A-loops, we measured k_{obs} and K_D^{app} on EA-KaiC containing the E444D substitution. Relative to EA-KaiC, for EA-KaiC^{E444D}, we found a complete reversal of A-loop burial ⇔ exposure and KaiA–KaiC affinities (Fig. 4). These data suggest that phosphoryl-S431-dependent burial of the A-loops imposes negative feedback regulation on the KaiA–KaiC interaction. This allosteric, KaiB-independent mechanism during the later part of the phosphorylation phase is likely to promote formation of the KaiA–KaiB–KaiC dephosphorylation complex.

KaiA–KaiB–KaiC cooperativity contributes to clock output

In order for circadian clocks to synchronize cellular processes to daily swings in ambient light and temperature, mechanisms must exist to transmit temporal information from the oscillator to other pathways. In cyanobacteria, two mutually antagonistic output pathways, initiated by the SasA and CikA proteins, transduce KaiC phosphorylation rhythms into genome-wide transcription rhythms [47,67]. SasA phosphorylates/activates the transcription factor RpaA, whereas CikA dephosphorylates/deactivates RpaA. SasA is a sensor histidine kinase [42] that, upon binding KaiC, phosphorylates [43] and then transfers the phosphoryl group to the transcription factor RpaA, thereby activating it [44,47,67]. Once activated, RpaA induces transcription of genes such as *kaiBC*. In this way, circadian rhythms of SasA activity drive genome-wide transcription rhythms. SasA binds directly to KaiC using its N-terminal domain [42]. Recently, it was found that KaiB and SasA compete for binding to KaiC [12,46], suggesting that KaiB plays a direct role in regulating clock output [12]. Since the formation of the KaiA–KaiB–KaiC complex is cooperative, we wanted to determine whether KaiA also plays a role in regulating SasA–KaiC interactions. We set up competition experiments between the isolated N-terminal domain of SasA, ^{N}SasA [68], and KaiB (or KaiB*) ± KaiA (or ±$^{\Delta N}$KaiA) (Fig. 5 and Fig. S4b and c). In order to minimize KaiA binding to the CII side [18,19], we used a construct of EE-KaiC missing its C-terminal extensions, EE-KaiC^{497} (Fig. 1a) [23]. We also tested ^{N}SasA and KaiB competition for binding CI*, which was recently identified as their binding site [23,24,45]. Because ^{N}SasA has no naturally occurring cysteinyl residues, a G57C substitution allowed labeling it with a thiol-reactive fluorophore so that competition could be monitored using fluorescence anisotropy. As seen in Fig. 5 and Fig. S4b and c, the fluorescence anisotropy of free ^{N}SasA was much lower than when it was bound to EE-KaiC^{497} or CI*, providing sufficient dynamic range for competition experiments. KaiB displaced ^{N}SasA slowly from EE-KaiC^{497} and CI*. The displacement was significantly faster in the presence of increasing concentration of KaiA [or $^{\Delta N}$KaiA (Fig. S4b and c)]. This observation demonstrates that KaiA enhances the competitiveness of KaiB over ^{N}SasA for KaiC. Therefore, through its role in the cooperativity of KaiA–KaiB–KaiC interactions, KaiA appears to modulate SasA–KaiC interactions, with implications for regulating clock output. Since KaiB* binds KaiC much faster than KaiB [24], it was not surprising that, even in the absence of KaiA, KaiB* quickly displaced ^{N}SasA (Fig. 5 and Fig. S4b and c).

SasA and KaiB bind to B-loops on CI

To better understand the basis of the competition between SasA and KaiB, we investigated whether they shared binding elements on CI. This identification was aided by sequence alignments between the highly similar [13] RecA-like [14] CI and CII domains of KaiC. As seen in Fig. 6a, CI contains an insertion of several residues (116–123) not found in CII. This insertion is exposed on the bottom of CI as part of a loop, which we

Fig. 6. ^{N}SasA and KaiB* compete on CI near the B-loops.(a) CLUSTAL-W multiple sequence alignment of the two domains of KaiC from different cyanobacteria species reveals an insertion in CI missing in CII. The insertion, termed the "B-loop", is from residues 116 to 123 (highlighted in yellow). Sequences correspond to the following strains: BP-1, *T. elongatus* BP-1 (used in this study); PCC-7942, *S. elongatus* PCC-7942; PCC-8801, *Synechococcus* sp. PCC-8801; PCC-9709, *Nostoc* sp. PCC-9709; IAM M-101, *Lentinula boryana* IAM M-101; FACHB-438, *Acanthastrea maxima* FACHB-438; PCC-7806, *Microcystis aeruginosa* PCC-7806.(b) Gel-filtration profiles of CI* + KaiB* (red, from Fig. 1a), CI* + ^{N}SasA (brown), CI*$^{\Delta}$ + KaiB* (orange), and CI*$^{\Delta}$ + ^{N}SasA (cyan). CI*$^{\Delta}$ is with B-loop (residues 116–123) deleted. Peaks denoted by *a*, *b*, *c*, *d*, *e*, *f*, *g*, and *h* were checked by SDS/PAGE. Molecular mass markers in kilodaltons are marked by black arrows along the top of the gel-filtration chromatograms. For details on the protein constructs and experimental setup, please see Table S1.(c) SDS/PAGE gel of peaks *a*, *b*, *c*, *d*, *e*, *f*, *g*, and *h* in (b).

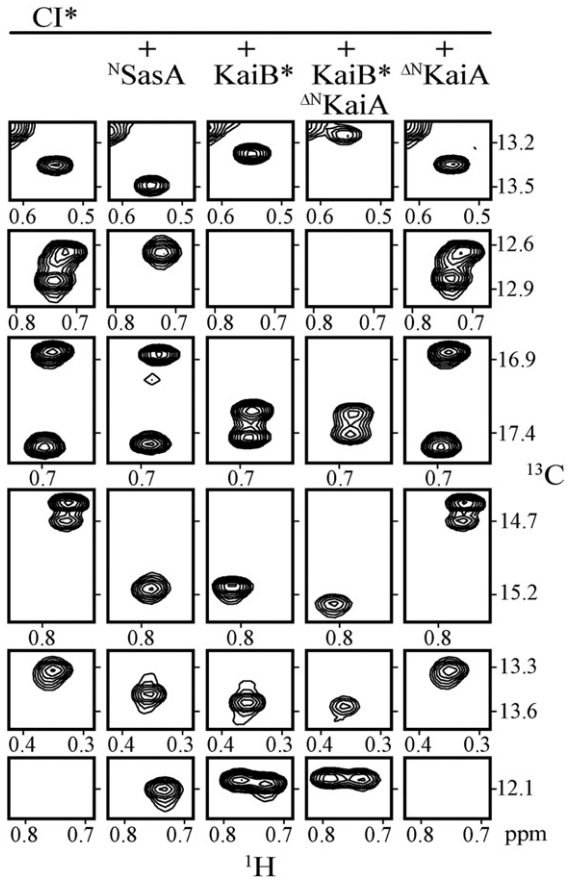

Fig. 7. ^{N}SasA and KaiB* do not interact identically with CI.Selected regions from methyl-TROSY spectra of U-[^{15}N, ^{2}H]-Ile-δ1-[^{13}C, ^{1}H]-labeled CI* alone (column 1), in the presence of ^{N}SasA (column 2), KaiB* (column 3), KaiB* + $^{\Delta N}$KaiA (column 4), or $^{\Delta N}$KaiA (column 5). Full spectra are shown in Fig. S7. For details on the protein constructs, please see Table S1.

named the B-loop (Fig. 1a). The construct, CI*$^{\Delta}$ (Fig. 1a), missing the B-loop insertion, retained the structure of CI*, as determined from a comparison of their NMR fingerprints (Fig. S5b). However, unlike with CI*, CI*$^{\Delta}$ could not bind ^{N}SasA or KaiB* (Fig. 6b). This result strongly suggests that the B-loop forms part of the binding site for both proteins. Although the binding sites of ^{N}SasA and KaiB on CI overlap, their interactions with CI are not identical, as suggested by a comparison of chemical shift perturbations induced by ^{N}SasA and KaiB* in methyl-TROSY spectra of U-[^{15}N, ^{2}H]-Ile-δ1-[^{13}C, ^{1}H]CI* (Fig. 7, rows 1–3).

Perturbations of CI* spectra by KaiB* were not significantly perturbed further by the addition of $^{\Delta N}$KaiA, and $^{\Delta N}$KaiA by itself did not perturb the spectrum of CI* (Fig. 7, columns 4 and 5), providing further support for the notion that sequestration of KaiA on CI likely does not involve direct KaiA–KaiC interactions but occurs indirectly through KaiA–KaiB interactions. Furthermore, it also suggests that CI

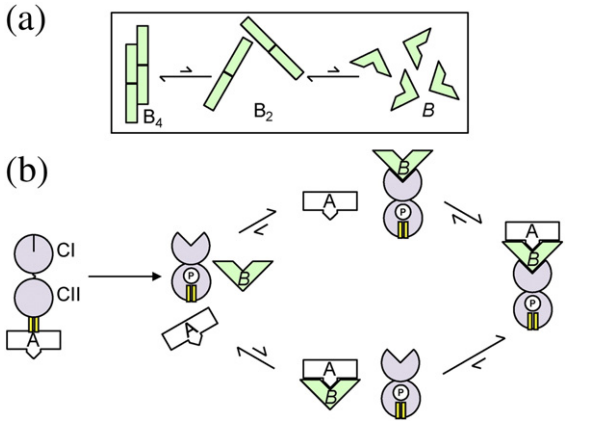

Fig. 8. Model of cooperative formation of the KaiABC dephosphorylation complex. (a) KaiB exists in a dynamic equilibrium between distinct quaternary states: tetramer (B_4), dimer (B_2), and active monomer (*B*). B_4 is the most stable form [55–57], whereas *B* is a highly transient state. (b) The CI domain of KaiC and KaiA can each stabilize the highly active monomer of KaiB, *B*, thereby cooperatively forming the KaiABC dephosphorylation complex. A-loops of KaiC are depicted as yellow bars. P indicates phosphorylation at S431 of KaiC. Upon S431 phosphorylation, two major allosteric events occur in KaiC: (1) The A-loops are shifted toward their buried position due to CII-ring tightening [23], and KaiA consequently loses affinity for the CII domain. (2) The CI and CII domains of KaiC stack together, exposing the KaiB binding site on CI [24]. Now, the CI domain can selectively capture the highly transient *B*, enhancing KaiA sequestration. Alternatively, KaiA can selectively capture *B*, thereby promoting binding to KaiC.

adopts the same conformation in the binary KaiB–KaiC and ternary KaiA–KaiB–KaiC complexes. These observations contradict recent studies suggesting that KaiB and SasA bind to the CII side of KaiC [61,69].

Discussion

Based upon our findings, we think that the most stable form of KaiB, the homotetramer [55–57], cannot bind KaiA or KaiC but is in a dynamic equilibrium with transiently disassociated subunits that can bind. Our previous demonstration of slow KaiB–KaiC binding, faster KaiB*–KaiC binding, and subunit shuffling between KaiB proteins supports this notion [24]. Significant changes in NMR spectra of KaiB* after hours of incubation with KaiA (Fig. S5a) also indicate that large changes in the tertiary structure of KaiB occur upon binding, reminiscent of KaiB–KaiC binding [24]. KaiA speeds up KaiB–KaiC binding by shifting KaiB away from the tetramer and toward KaiB subunits active in binding KaiC. In the same way, KaiC enhances the KaiA–KaiB interaction. Thus, formation of the KaiA–KaiB–

KaiC dephosphorylation complex on the CI side of KaiC is cooperative. This cooperativity is probably aided by KaiB-independent negative feedback imposed on the KaiA–KaiC interaction on the CII side of KaiC toward the end of the phosphorylation phase. We present our model of the KaiA–KaiB–KaiC interaction in Fig. 8.

Based on EM data, it has been suggested that the competition between SasA and KaiB is on the CII domain of KaiC [61], instead of CI as we propose. The low resolution of the EM data of KaiC makes it difficult to unambiguously distinguish the CI from CII domains, in our opinion. In support of CI binding, another group has independently verified that SasA binds to CI [45]. Additionally, the Rust group showed that the ATPase activity in the CI ring of KaiC was essential for KaiB-KaiC binding [58]. We think that this ATPase activity is dependent on CI-CII ring-stacking interactions, and may be important for exposing the KaiB–binding site [24]. Our identification of the B-loop of CI as a common element of the KaiB and SasA binding sites adds further support that these interactions take place on CI. Also, NMR spectra of the KaiB*–CI* and ^{N}SasA–CI* complexes (Fig. 7 and Figs. S5c and S7) argue against artifactual interactions.

Since our data suggest that a single subunit of KaiB binds to a dimer of KaiA, it was important to see how well this stoichiometry agreed with published results, using back-of-the-envelope calculations. It has been shown that KaiB complexation (KaiA–KaiB–KaiC and KaiB–KaiC complexes) lags KaiC phosphorylation by 4–8 h [11,63,70]. When these complexes reach peak levels (at t_{max} in Fig. S8), ~60% of total KaiB is bound [11]. A new cycle of phosphorylation does not initiate until at least half of these complexes have disassociated (at $t_{1/2}$ in Fig. S8) [11]. Thus, from $t_{max} \rightarrow t_{1/2}$, KaiA that is desequestered from decomposition of KaiA–KaiB–KaiC complexes would need to be resequestered by intact KaiBC complexes to prevent premature phosphorylation. Using the known dependency of the phosphorylation rhythm on KaiA and KaiB concentrations [71], by our estimation, resequestration is possible when using a stoichiometry of one monomeric subunit of KaiB binding one dimer of KaiA (Table S2 and Fig. S8). In contrast, resequestration of desequestered KaiA from $t_{max} \rightarrow t_{1/2}$ was not possible when we assumed that a dimer of KaiB sequestered a KaiA dimer [49] or monomer [46]. Thus, the literature lends support to our model. In conclusion, the circadian oscillator of cyanobacteria uses cooperativity to reciprocally regulate periodic formation of complexes on the CI and CII rings of KaiC. This cooperativity likely influences downstream output signaling as well. Thus, understanding the dynamic and allosteric mechanism of the oscillator is an important first step in elucidating how it transduces clock output signals.

Materials and Methods

Protein expression and purification

T. elongatus kaiA, *kaiB*, and *kaiC* genes were cloned into pET-28b by PCR using the NdeI/HindIII sites as described previously [24]. Table S1 presents the abbreviations and complete names of the proteins and corresponding constructs. Proteins were expressed in BL21(DE3) *Escherichia coli* (Novagen) and purified by Ni-NTA affinity chromatography and size-exclusion chromatography as described previously [24], except KaiC proteins were expressed in M9 (H_2O) minimal medium with $^{14}NH_4Cl$ for higher purity and yield. Details are provided in Supplementary Material.

Analytical gel-filtration chromatography

All gel-filtration chromatography experiments were performed with a Superdex 200 10/300 GL column (GE Healthcare) as described previously [24], except that the sample injection volume was 250 μL. Details of experimental setup and proteins used in each experiment are provided in Supplementary Material.

Fluorescence spectroscopy

All data were measured with an ISS PC1 spectrofluorometer. The thiol-reactive fluorophores used for all experiments were 6-iodoacetamidofluorescein (6-IAF) (Invitrogen). The excitation and emission wavelengths were 492 nm and 530 nm, respectively. Data were fit to a single exponential equation with Mathematica software (Wolfram). Details of experimental setup and proteins used in each experiment are provided in Supplementary Material.

A-loop proteolysis reactions

Each of the five KaiC phosphomimic variants (AA-KaiC, AE-KaiC, EE-KaiC, EA-KaiC, EA-KaiC^{E444D}) with a thrombin cut site (LVPRGS) replacing residues I497–K502 was incubated with thrombin at 30 °C. Aliquots were obtained at indicated time points for SDS/PAGE analysis. Following electrophoresis of 60 V for 30 min and 140 V for 120 min, we stained gels with Coomassie brilliant blue R250 (EMD Chemicals) and determined the percentages of cut product over total protein by densitometry using ImageJ (National Institutes of Health) and PeakFit (SeaSolve Software). k_{obs} values were determined by fitting the thrombin digest kinetics to a single exponential equation using Mathematica software. Details of experimental setup and proteins used in each experiment are provided in Supplementary Material.

In vitro KaiC phosphorylation reactions

Experimental setup was as described previously [24], except that 5 μM KaiC was incubated with 5 μM KaiB and 1.67 μM KaiA or $^{\Delta N}$KaiA at 35 °C. Approximately 100 μL of

transparent mineral oil (CMP 25; Cambridge Mill Products, Inc.) was layered on top of the reaction solution to prevent evaporation. Aliquots were obtained at indicated time points for SDS/PAGE analysis. Following electrophoresis as described previously [24], gels were stained with Coomassie brilliant blue R250 (EMD Chemicals), and the percentage of KaiC phosphorylation was determined by densitometry using ImageJ (National Institutes of Health) and PeakFit (SeaSolve Software). Details of experimental setup and proteins used in each experiment are provided in Supplementary Material.

NMR spectroscopy

All NMR experiments were run on a Bruker 600-MHz AVANCE III spectrometer equipped with a TCI cryoprobe. Spectra were processed and analyzed using NMRPipe and NMRDraw [72]. Details of experimental setup and proteins used in each experiment are provided in Supplementary Material.

Acknowledgements

This research was supported by a grant (W911NF-10-1-0090) from the Army. R.T. was supported by a National Science Foundation Graduate Research Fellowship.

Appendix A. Supplementary data

Supplementary data to this article can be found online at http://dx.doi.org/10.1016/j.jmb.2013.09.040.

Received 16 April 2013;
Received in revised form 22 August 2013;
Accepted 27 September 2013
Available online 07 October 2013

Keywords:
cooperativity;
phosphorylation;
NMR;
protein;
fluorescence

Abbreviations used:
EM, electron microscopy; 6-IAF, 6-iodoacetamidofluorescein.

References

[1] Dunlap JC, Loros JJ, DeCoursey PJ. Chronobiology: biological timekeeping. Sunderland, MA: Sinauer Associates, Inc.; 2004.
[2] Jeyaraj D, Haldar SM, Wan X, McCauley MD, Ripperger JA, Hu K, et al. Circadian rhythms govern cardiac repolarization and arrhythmogenesis. Nature 2012;483:96–9.
[3] Woelfle MA, Ouyang Y, Phanvijhitsiri K, Johnson CH. The adaptive value of circadian clocks: an experimental assessment in cyanobacteria. Curr Biol 2004;14:1481–6.
[4] Oliver P, Sobczyk M, Maywood E, Edwards B, Lee S, Livieratos A, et al. Disrupted circadian rhythms in a mouse model of schizophrenia. Curr Biol 2012;22:314–9.
[5] Goodspeed D, Chehab EW, Min-Venditti A, Braam J, Covington MF. Arabidopsis synchronizes jasmonate-mediated defense with insect circadian behavior. Proc Natl Acad Sci 2012;109:4674–7.
[6] Bass J. Circadian topology of metabolism. Nature 2012;491:348–56.
[7] Masri S, Sassone-Corsi P. The circadian clock: a framework linking metabolism, epigenetics and neuronal function. Nat Rev Neurosci 2013;14:69–75.
[8] Ishiura M, Kutsuna S, Aoki S, Iwasaki H, Andersson CR, Tanabe A, et al. Expression of a gene cluster *kaiABC* as a circadian feedback process in cyanobacteria. Science 1998;281:1519–23.
[9] Nakajima M, Imai K, Ito H, Nishiwaki T, Murayama Y, Iwasaki H, et al. Reconstitution of circadian oscillation of cyanobacterial KaiC phosphorylation *in vitro*. Science 2005;308:414–5.
[10] Yoshida T, Murayama Y, Ito H, Kageyama H, Kondo T. Nonparametric entrainment of the *in vitro* circadian phosphorylation rhythm of cyanobacterial KaiC by temperature cycle. Proc Natl Acad Sci 2009;106:1648–53.
[11] Goda K, Ito H, Kondo T, Oyama T. Fluorescence correlation spectroscopy to monitor Kai protein-based circadian oscillations in real time. J Biol Chem 2012;287:3241–8.
[12] Murakami R, Mutoh R, Iwase R, Furukawa Y, Imada K, Onai K, et al. The roles of the dimeric and tetrameric structures of the clock protein KaiB in the generation of circadian oscillations in cyanobacteria. J Biol Chem 2012;287:29506–15.
[13] Iwasaki H, Taniguchi Y, Ishiura M, Kondo T. Physical interactions among circadian clock proteins KaiA, KaiB, and KaiC in cyanobacteria. EMBO J 1999;18:1137–45.
[14] Leipe DD, Aravind L, Grishin NV, Koonin EV. The bacterial replicative helicase DnaB evolved from a RecA duplication. Genome Res 2000;10:5–16.
[15] Pattanayek R, Mori T, Xu Y, Pattanayek S, Johnson CH, Egli M. Structures of KaiC circadian clock mutant proteins: a new phosphorylation site at T426 and mechanisms of kinase, ATPase and phosphatase. PLoS One 2009;4:e7529.
[16] Pattanayek R, Wang J, Mori T, Xu Y, Johnson CH, Egli M. Visualizing a circadian clock protein: crystal structure of KaiC and functional insights. Mol Cell 2004;15:375–88.
[17] Williams SB, Vakonakis I, Golden SS, LiWang A. Structure and function from the circadian clock protein KaiA of *Synechococcus elongatus*: a potential clock input mechanism. Proc Natl Acad Sci USA 2002;99:15357–62.
[18] Kim Y, Dong G, Carruthers CW, Golden SS, LiWang A. The day/night switch in KaiC, a central oscillator component of the circadian clock of cyanobacteria. Proc Natl Acad Sci USA 2008;105:12825–30.
[19] Pattanayek R, Williams DR, Pattanayek S, Xu Y, Mori T, Johnson CH, et al. Analysis of KaiA–KaiC protein interactions in the cyanobacterial circadian clock using hybrid structural methods. EMBO J 2006;25:2017–28.
[20] Vakonakis I, LiWang A. Structure of the C-terminal domain of the clock protein KaiA in complex with a KaiC-derived peptide:

implications for KaiC regulation. Proc Natl Acad Sci USA 2004;101:10925–30.
[21] Rust MJ, Markson JS, Lane WS, Fisher DS, O'Shea EK. Ordered phosphorylation governs oscillation of a three-protein circadian clock. Science 2007;318:809–12.
[22] Nishiwaki T, Satomi Y, Kitayama Y, Terauchi K, Kiyohara R, Takao T, et al. A sequential program of dual phosphorylation of KaiC as a basis for circadian rhythm in cyanobacteria. EMBO J 2007;26:4029–37.
[23] Chang Y, Kuo N, Tseng R, LiWang A. Flexibility of the C-terminal, or CII, ring of KaiC governs the rhythm of the circadian clock of cyanobacteria. Proc Natl Acad Sci USA 2011;108:14431–6.
[24] Chang Y, Tseng R, Kuo N, LiWang A. Rhythmic ring-ring stacking drives the circadian oscillator clockwise. Proc Natl Acad Sci USA 2012;109:16847–51.
[25] Nishiwaki T, Kondo T. The circadian autodephosphorylation of cyanobacterial clock protein KaiC occurs via the formation of ATP as an intermediate. J Biol Chem 2012;287:18030–5.
[26] Egli M, Mori T, Pattanayek R, Xu Y, Qin X, Johnson CH. Dephosphorylation of the core clock protein KaiC in the cyanobacterial KaiABC circadian oscillator proceeds via an ATP synthase mechanism. Biochemistry 2012;51:1547–58.
[27] Kim Y, Vinyard DJ, Ananyev GM, Dismukes GC, Golden SS. Oxidized quinones signal onset of darkness directly to the cyanobacterial circadian oscillator. Proc Natl Acad Sci 2012;109:17765–9.
[28] Ivleva NB, Gao T, LiWang A, Golden SS. Quinone sensing by the circadian input kinase of the cyanobacterial circadian clock. Proc Natl Acad Sci USA 2006;103:17468–73.
[29] Wood TL, Bridwell-Rabb J, Kim Y, Gao T, Chang Y, LiWang A, et al. The KaiA protein of the cyanobacterial circadian oscillator is modulated by a redox-active cofactor. Proc Natl Acad Sci USA 2010;107:5804–9.
[30] Pattanayek R, Sidiqi SK, Egli M. Crystal structure of the redox-active cofactor dibromothymoquinone bound to circadian clock protein KaiA and structural basis for dibromothymoquinone's ability to prevent stimulation of KaiC phosphorylation by KaiA. Biochemistry 2012;51:8050–2.
[31] Schmitz O, Katayama M, Williams SB, Kondo T, Golden SS. CikA, a bacteriophytochrome that resets the cyanobacterial circadian clock. Science 2000;289:765–8.
[32] Mackey SR, Choi J, Kitayama Y, Iwasaki H, Dong G, Golden SS. Proteins found in a CikA interaction assay link the circadian clock, metabolism, and cell division in *Synechococcus elongatus*. J Bacteriol 2008;190:3738–46.
[33] Zhang X, Dong G, Golden SS. The pseudo-receiver domain of CikA regulates the cyanobacterial circadian input pathway. Mol Microbiol 2006;60:658–68.
[34] Gao T, Zhang X, Ivleva NB, Golden SS, LiWang A. NMR structure of the pseudo-receiver domain of CikA. Protein Sci 2007;16:465–75.
[35] Rust MJ, Golden SS, O'Shea EK. Light-driven changes in energy metabolism directly entrain the cyanobacterial circadian oscillator. Science 2011;331:220–3.
[36] Liu Y, Tsinoremas N, Johnson C, Lebedeva N, Golden SS, Ishiura M, et al. Circadian orchestration of gene expression in cyanobacteria. Genes Dev 1995;9:1469–78.
[37] Ito H, Mutsuda M, Murayama Y, Tomita J, Hosokawa N, Terauchi K, et al. Cyanobacterial daily life with Kai-based circadian and diurnal genome-wide transcriptional control in *Synechococcus elongatus*. Proc Natl Acad Sci 2009;106:14168–73.
[38] Vijayan V, Zuzow R, O'Shea EK. Oscillations in supercoiling drive circadian gene expression in cyanobacteria. Proc Natl Acad Sci USA 2009;106:22564–8.
[39] Nakahira Y, Katayama M, Miyashita H, Kutsuna S, Iwasaki H, Oyama T, et al. Global gene repression by KaiC as a master process of prokaryotic circadian system. Proc Natl Acad Sci USA 2004;101:881–5.
[40] Dong G, Yang Q, Wang Q, Kim Y, Wood TL, Osteryoung KW, et al. Elevated ATPase activity of KaiC applies a circadian checkpoint on cell division in *Synechococcus elongatus*. Cell 2010;140:529–39.
[41] Yang Q, Pando BF, Dong G, Golden SS, van Oudenaarden A. Circadian gating of the cell cycle revealed in single cyanobacterial cells. Science 2010;327:1522–6.
[42] Iwasaki H, Williams SB, Kitayama Y, Ishiura M, Golden SS, Kondo T. A KaiC-interacting sensory histidine kinase, SasA, necessary to sustain robust circadian oscillation in cyanobacteria. Cell 2000;101:223–33.
[43] Smith RM, Williams SB. Circadian rhythms in gene transcription imparted by chromosome compaction in the cyanobacterium *Synechococcus elongatus*. Proc Natl Acad Sci USA 2006;103:8564–9.
[44] Takai N, Nakajima M, Oyama T, Kito R, Sugita C, Sugita M, et al. A KaiC-associating SasA–RpaA two-component regulatory system as a major circadian timing mediator in cyanobacteria. Proc Natl Acad Sci USA 2006;103:12109–14.
[45] Valencia SJ, Bitou K, Ishii K, Murakami R, Morishita M, Onai K, et al. Phase-dependent generation and transmission of time information by the KaiABC circadian clock oscillator through SasA-KaiC interaction in cyanobacteria. Genes Cells 2012;17:398–419.
[46] Pattanayek R, Williams DR, Rossi G, Weigand S, Mori T, Johnson CH, et al. Combined SAXS/EM based models of the *S. elongatus* post-translational circadian oscillator and its interactions with the output His-kinase SasA. PLoS One 2011;6:e23697.
[47] Gutu A, O'Shea E. Two antagonistic clock-regulated histidine kinases time the activation of circadian gene expression. Mol Cell 2013;50:288–94.
[48] Iwasaki H, Nishiwaki T, Kitayama Y, Nakajima M, Kondo T. KaiA-stimulated KaiC phosphorylation in circadian timing loops in cyanobacteria. Proc Natl Acad Sci USA 2002;99:15788–93.
[49] Mutoh R, Mino H, Murakami R, Uzumaki T, Takabayashi A, Ishii K, et al. Direct interaction between KaiA and KaiB revealed by a site-directed spin labeling electron spin resonance analysis. Genes Cells 2010;15:269–80.
[50] Golden SS, Ishiura M, Johnson CH, Kondo T. Cyanobacterial circadian rhythms. Annu Rev Plant Physiol Plant Mol Biol 1997;48:327–54.
[51] Garces RG, Wu N, Gillon W, Pai EF. Anabaena circadian clock proteins KaiA and KaiB reveal a potential common binding site to their partner KaiC. EMBO J 2004;23:1688–98.
[52] Uzumaki T, Fujita M, Nakatsu T, Hayashi F, Shibata H, Itoh N, et al. Crystal structure of the C-terminal clock-oscillator domain of the cyanobacterial KaiA protein. Nat Struct Mol Biol 2004;11:623–31.
[53] Sprangers R, Kay LE. Quantitative dynamics and binding studies of the 20S proteasome by NMR. Nature 2007;445:618–22.
[54] Qin X, Byrne M, Mori T, Zou P, Williams DR, Mchaourab H, et al. Intermolecular associations determine the dynamics of the circadian KaiABC oscillator. Proc Natl Acad Sci USA 2010;107:14805–10.

[55] Pattanayek R, Williams DR, Pattanayek S, Mori T, Johnson CH, Stewart PL, et al. Structural model of the circadian clock KaiB–KaiC complex and mechanism for modulation of KaiC phosphorylation. EMBO J 2008;27:1767–78.
[56] Hitomi K, Oyama T, Han S, Arvai AS, Getzoff ED. Tetrameric architecture of the circadian clock protein KaiB: a novel interface for intermolecular interactions and its impact on the circadian rhythm. J Biol Chem 2005;280:19127–35.
[57] Iwase R, Imada K, Hayashi F, Uzumaki T, Morishita M, Onai K, et al. Functionally important substructures of circadian clock protein KaiB in a unique tetramer complex. J Biol Chem 2005;280:43141–9.
[58] Phong C, Markson JS, Wilhoite CM, Rust MJ. Robust and tunable circadian rhythms from differentially sensitive catalytic domains. Proc Natl Acad Sci 2013;110:1124–9.
[59] Ye S, Vakonakis I, Ioerger TR, LiWang A, Sacchettini JC. Crystal structure of circadian clock protein KaiA from *Synechococcus elongatus*. J Biol Chem 2004;279:20511–8.
[60] Vakonakis I, Sun J, Wu T, Holzenburg A, Golden SS, LiWang A. NMR structure of the KaiC-interacting C-terminal domain of KaiA, a circadian clock protein: implications for the KaiA-KaiC interaction. Proc Natl Acad Sci USA 2004;101:1479–84.
[61] Pattanayek R, Yadagirl KK, Ohi MD, Egli M. Nature of KaiB-KaiC binding in the cyanobacterial circadian oscillator. Cell Cycle 2013;12:810–7.
[62] Hayashi F, Ito H, Fujita M, Iwase R, Uzumaki T, Ishiura M. Stoichiometric interactions between cyanobacterial clock proteins KaiA and KaiC. Biochem Biophys Res Commun 2004;316:195–202.
[63] Ma L, Ranganathan R. Quantifying the rhythm of KaiB-C interaction for *in vitro* cyanobacterial circadian clock. PLoS One 2012;7:e42581.
[64] van Zon JS, Lubensky DK, Altena PRH, ten Wolde PR. An allosteric model of circadian KaiC phosphorylation. Proc Natl Acad Sci USA 2007;104:7420–5.
[65] Murayama Y, Mukaiyama A, Imai K, Onoue Y, Tsunoda A, Nohara A, et al. Tracking and visualizing the circadian ticking of the cyanobacterial clock protein KaiC in solution. EMBO J 2011;30:68–78.
[66] Terauchi K, Kitayama Y, Nishiwaki T, Miwa K, Murayama Y, Oyama T, et al. ATPase activity of KaiC determines the basic timing for circadian clock of cyanobacteria. Proc Natl Acad Sci USA 2007;104:16377–81.
[67] Taniguchi Y, Takai N, Katayama M, Kondo T, Oyama T. Three major output pathways from the KaiABC-based oscillator cooperate to generate robust circadian kaiBC expression in cyanobacteria. Proc Natl Acad Sci USA 2010;107:3263–8.
[68] Vakonakis I, Klewer DA, Williams SB, Golden SS, LiWang AC. Structure of the N-terminal domain of the circadian clock-associated histidine kinase SasA. J Mol Biol 2004;342:9–17.
[69] Villarreal SA, Pattanayek R, Williams DR, Mori T, Qin X, Johnson CH, et al. CryoEM and molecular dynamics of the circadian KaiB–KaiC complex indicates that KaiB monomers interact with KaiC and block ATP binding clefts. J Mol Biol 2013;425:3311–24.
[70] Kageyama H, Nishiwaki T, Nakajima M, Iwasaki H, Oyama T, Kondo T. Cyanobacterial circadian pacemaker: Kai protein complex dynamics in the KaiC phosphorylation cycle *in vitro*. Mol Cell 2006;23:161–71.
[71] Nakajima M, Ito H, Kondo T. *In vitro* regulation of circadian phosphorylation rhythm of cyanobacterial clock protein KaiC by KaiA and KaiB. FEBS Lett 2010;584:898–902.
[72] Delaglio F, Grzesiek S, Vuister GW, Zhu G, Pfeifer J, Bax A. NMRPipe: a multidimensional spectral processing system based on UNIX pipes. J Biomol NMR 1995;6:277–93.

Supplementary Material for

Cooperative KaiA–KaiB–KaiC interactions affect KaiB/SasA competition in the circadian clock of cyanobacteria

Roger Tseng[1,2], Yong-Gang Chang[1], Ian Bravo[1], Robert Latham[1], Abdullah Chaudhary[3], Nai-Wei Kuo[1], Andy LiWang[1,2,4,5]

Affiliations:

[1]School of Natural Sciences, University of California, Merced, CA 95343, USA.

[2]Quantitative and Systems Biology Graduate Group, University of California, Merced, CA 95343, USA.

[3]School of Engineering, University of California, Merced, CA 95343, USA.

[4]Chemistry and Chemical Biology, of California, Merced, CA 95343, USA.

[5]Center for Chronobiology, Division of Biological Sciences, University of California, San Diego, La Jolla, CA 92093, USA

*To whom correspondence should be addressed.

Andy LiWang

5200 North Lake Road, Merced, CA 95343

Telephone: (209) 228-4617

E-mail: aliwang@ucmerced.edu

Contents

Supplemental Figures

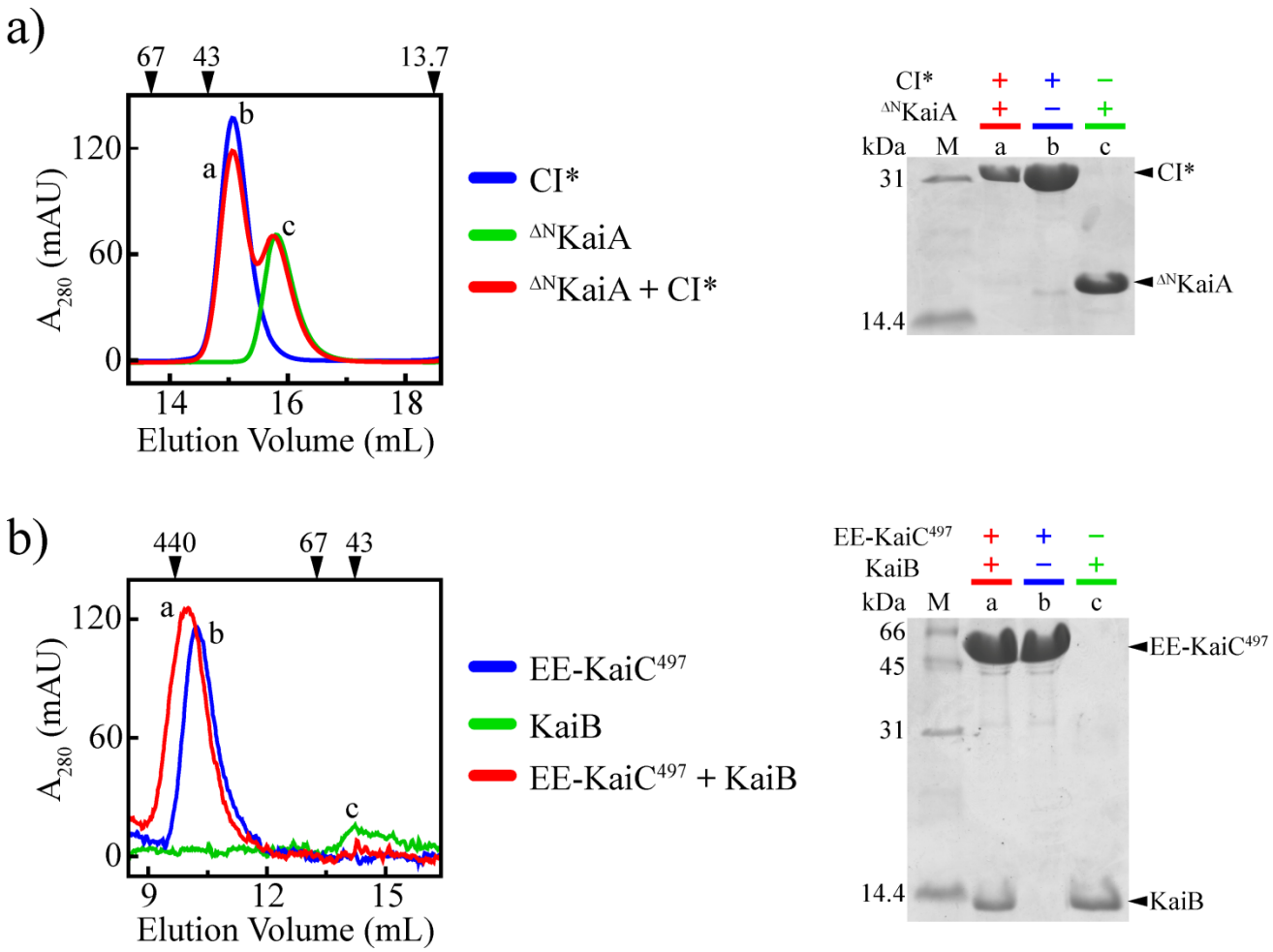

Fig. S1.

Gel filtration chromatograms show that (a) $^{\Delta N}$KaiA and CI* have no detectable interaction, and (b) wild-type KaiB interacts, as expected, with EE-KaiC^{497} (C-terminal truncation after residue I497). SDS/PAGE analysis of the chromatographic peaks in (a) and (b) are shown on the right. For details on the protein constructs and experimental setup, please see Table S1.

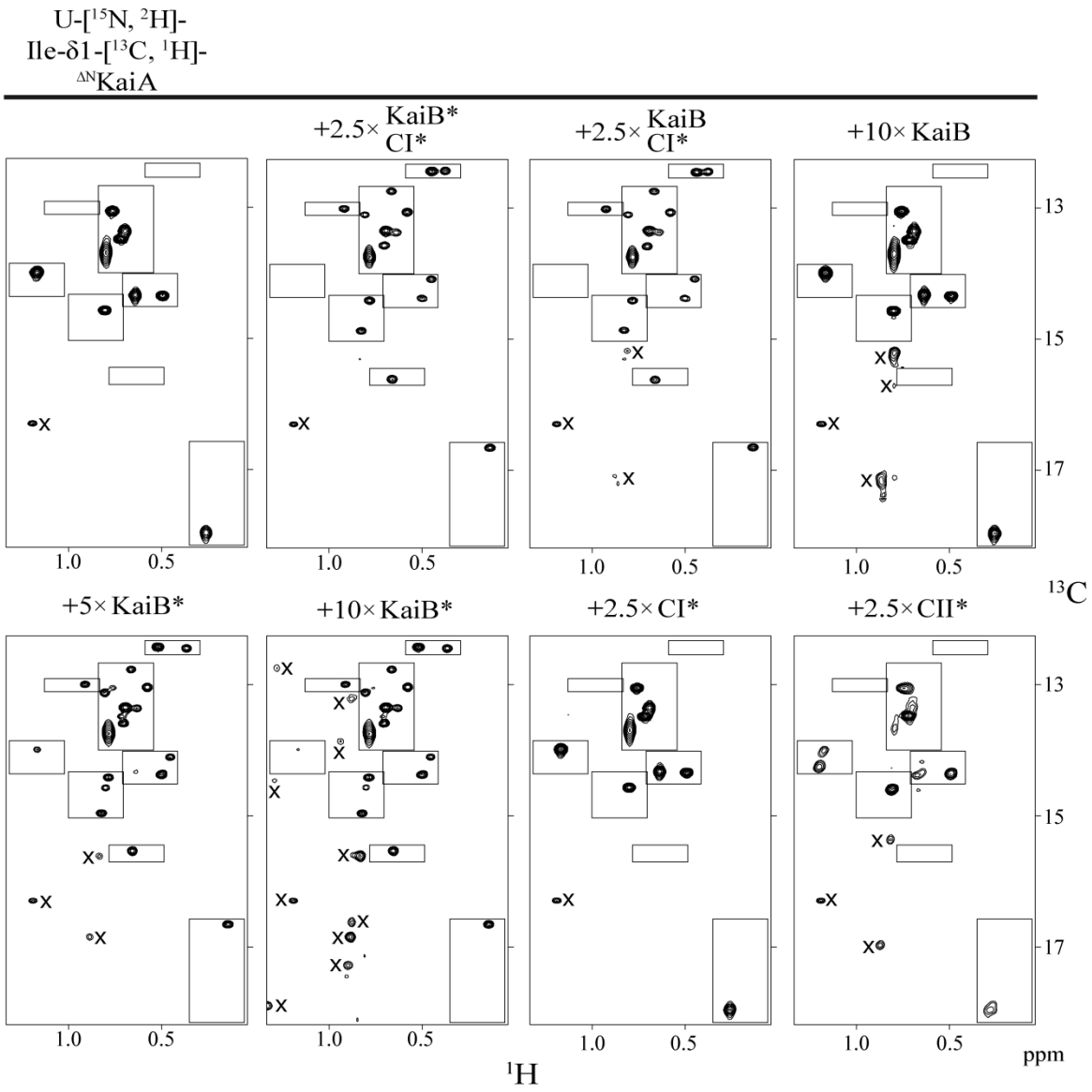

Fig. S2.

Methyl-TROSY spectra of U-[^{15}N, ^{2}H]-Ile-δ1-[^{13}C, ^{1}H]–labeled 1× $^{\Delta N}$KaiA alone (*top panel 1*), or in the presence of 2.5× (KaiB* + CI*) (*top panel 2*); 2.5× (KaiB + CI*) (*top panel 3*), 10× KaiB (*top panel 4*); 5× KaiB* (*bottom panel 1*); 10× KaiB (*bottom panel 2*); 2.5× CI* (*bottom panel 3*); or 2.5× CII* (*bottom panel 4*). 1× corresponds to 20 μM monomer concentration. Boxed regions are shown in main text Fig. 3a. All spectra were recorded with identical parameters, processed identically, and plotted at the same contour level. "X"s in all spectra mark aliased peaks that were also present in spectra of unlabeled control samples (data not shown). Thus, they are not Ile-δ1 methyl peaks belonging to labeled $^{\Delta N}$KaiA. For details on the protein constructs and experimental setup, please see Table S1.

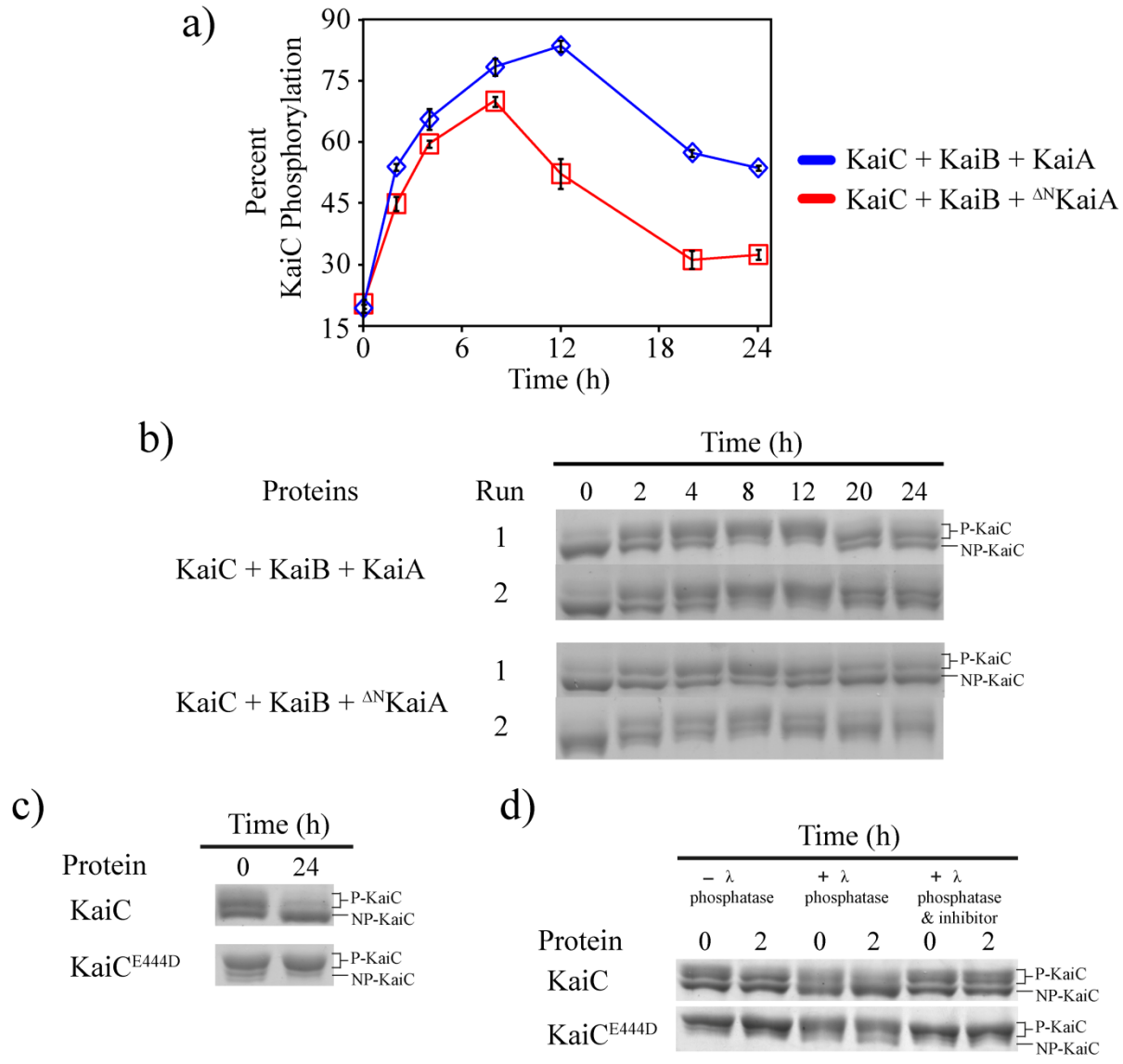

Fig. S3.

In vitro KaiC phosphorylation and dephosphorylation reactions. (a) 24-hour phosphorylation profiles of wild-type KaiA + KaiB + KaiC (blue) and $^{\Delta N}$KaiA + KaiB + KaiC (red) mixtures. Standard error was estimated from duplicate runs. (b) SDS/PAGE of KaiC phosphorylation time points, which were used for densitometry analysis in (a). P-KaiC and NP-KaiC stand for phosphorylated and non-phosphorylated KaiC, respectively. (c) Dephosphorylation of KaiC and KaiC^{E444D} over 24 hours. (d) Dephosphorylation of KaiC and KaiC^{E444D} over 2 hours ± lambda phosphatase ± inhibitor. For details on the protein constructs and experimental setup, please see Table S1 and page 21 of Supplementary Material.

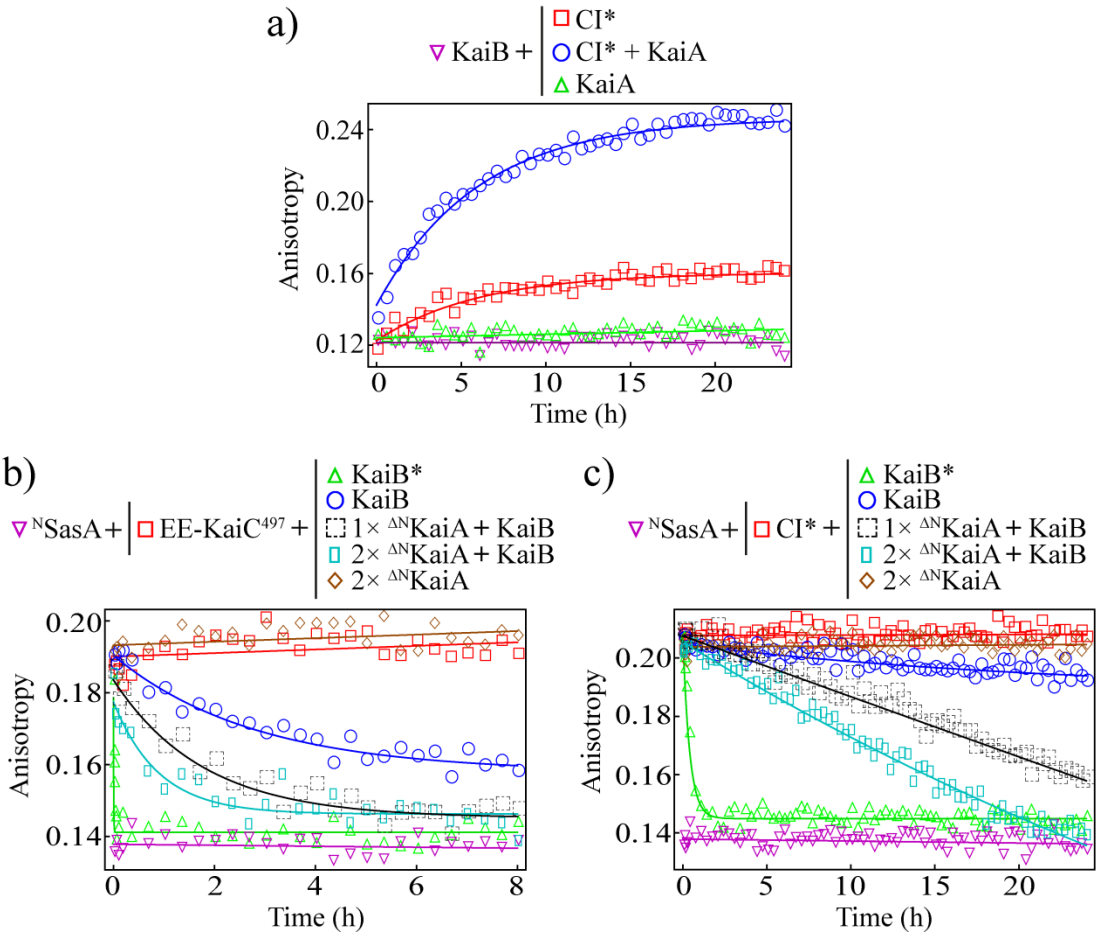

Fig. S4.

KaiA enhances KaiB-KaiC binding and competition of KaiB over SasA for KaiC. (a) Kinetics of 6-IAF labeled KaiB binding to CI*, CI* + KaiA, and KaiA over 24 hours by fluorescence anisotropy. Data were fit to equation (3) on page 19 of Supplementary Material, yielding k_{obs} values (h^{-1}) of 0.17 and 0.17 for CI* and CI* + KaiA, respectively. (b) and (c) are time courses of 6-IAF labeled ^{N}SasA-containing mixtures to which either EE-KaiC^{497} (left panel) or CI* (right panel) were added, as follows: buffer (red), 2× $^{\Delta N}$KaiA (brown), KaiB (blue), KaiB + 1× $^{\Delta N}$KaiA (black), KaiB + 2× $^{\Delta N}$KaiA (cyan), and KaiB* (green). Purple was used for data collected on a solution containing 6-IAF labeled ^{N}SasA as the sole protein component. Note that the only difference between (b) and (c) and Fig. 5 is that $^{\Delta N}$KaiA was used instead of KaiA. Data were fit to equation (4) in Supplementary Material, yielding k_{obs} values (h^{-1}) for (b)/(c) as follows: 0.36/nd, 0.56/nd, 1.12/nd, and 179/2.47 for KaiB, KaiB + 1x $^{\Delta N}$KaiA, KaiB + 2x $^{\Delta N}$KaiA, and KaiB*, respectively (nd is not determined). 1× corresponds to 10 μM monomer concentration. For details on the protein constructs and experimental setup, please see Table S1 and page 20 of Supplementary Material. For comparison, k_{obs} values (h^{-1}) for main text Fig. 5 (a)/(b) as follows: 0.38/nd and 1.02/nd for KaiB + 1x KaiA and KaiB + 2x KaiA, respectively.

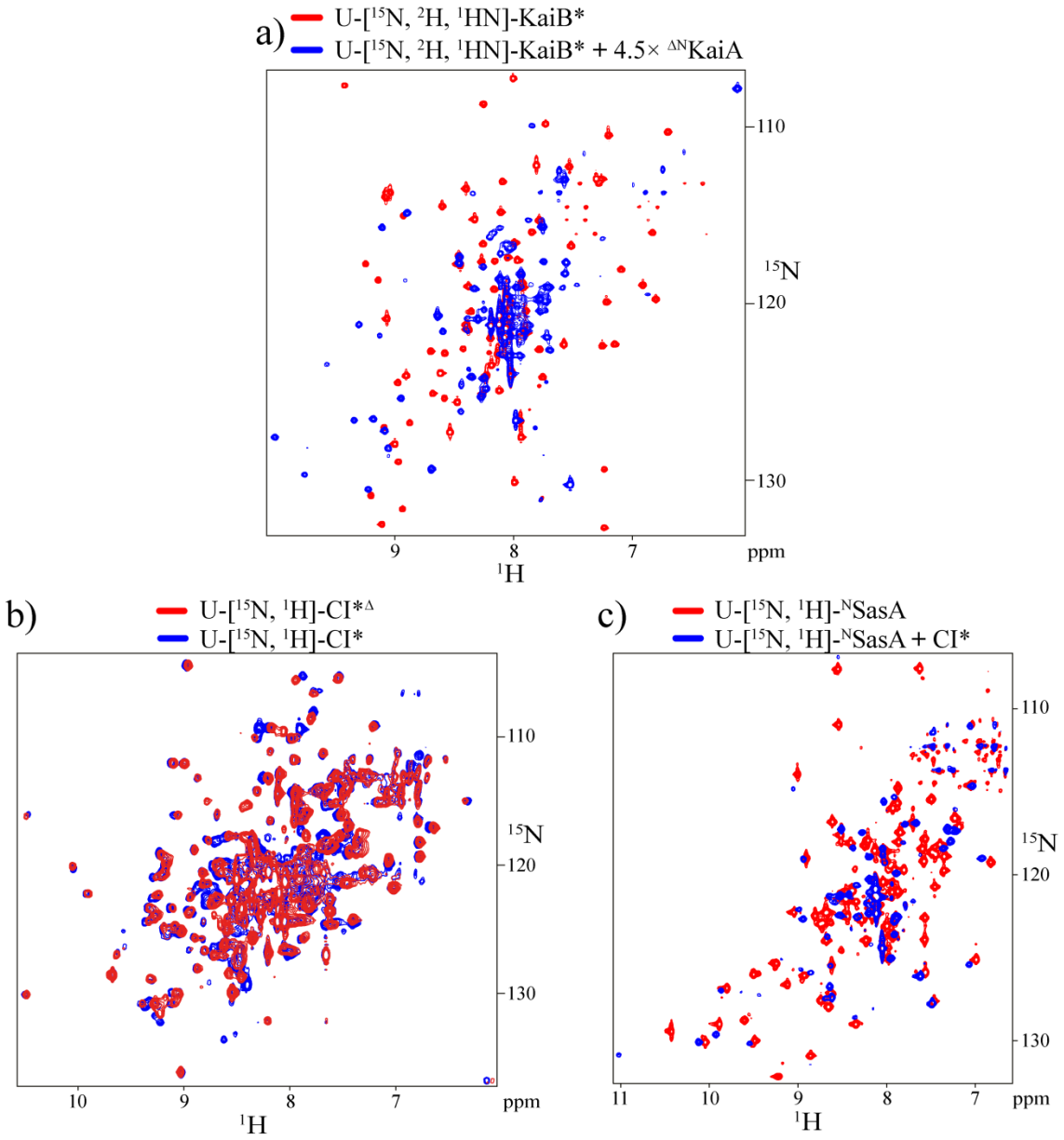

Fig. S5.

(a) Overlay of ^{15}N, ^{1}H-TROSY spectra of U-[^{15}N, ^{2}H, ^{1}H^{N}]-KaiB* free, with approximately 94 peaks (red), and in complex with 4.5× unlabeled $^{\Delta N}$KaiA, with approximately with 87 peaks (blue). There are 95 possible peaks for KaiB* (102 minus 7 prolines). 1× corresponds to 150 μM monomer concentration. No peaks corresponding to free KaiB* were observed under this saturating condition. (b) Overlay of ^{15}N, ^{1}H-TROSY spectra of U-[^{15}N, ^{1}H] labeled CI*$^{\Delta}$ (red) and CI* (blue), demonstrating that the "B-loop" deletion mutant CI*$^{\Delta}$ is still well folded and similar to CI*. (c) Overlay of ^{15}N, ^{1}H-TROSY spectra of U-[^{15}N, ^{1}H] labeled ^{N}SasA free (red) and bound to CI* (blue). For details on the protein constructs and experimental setup, please see Table S1.

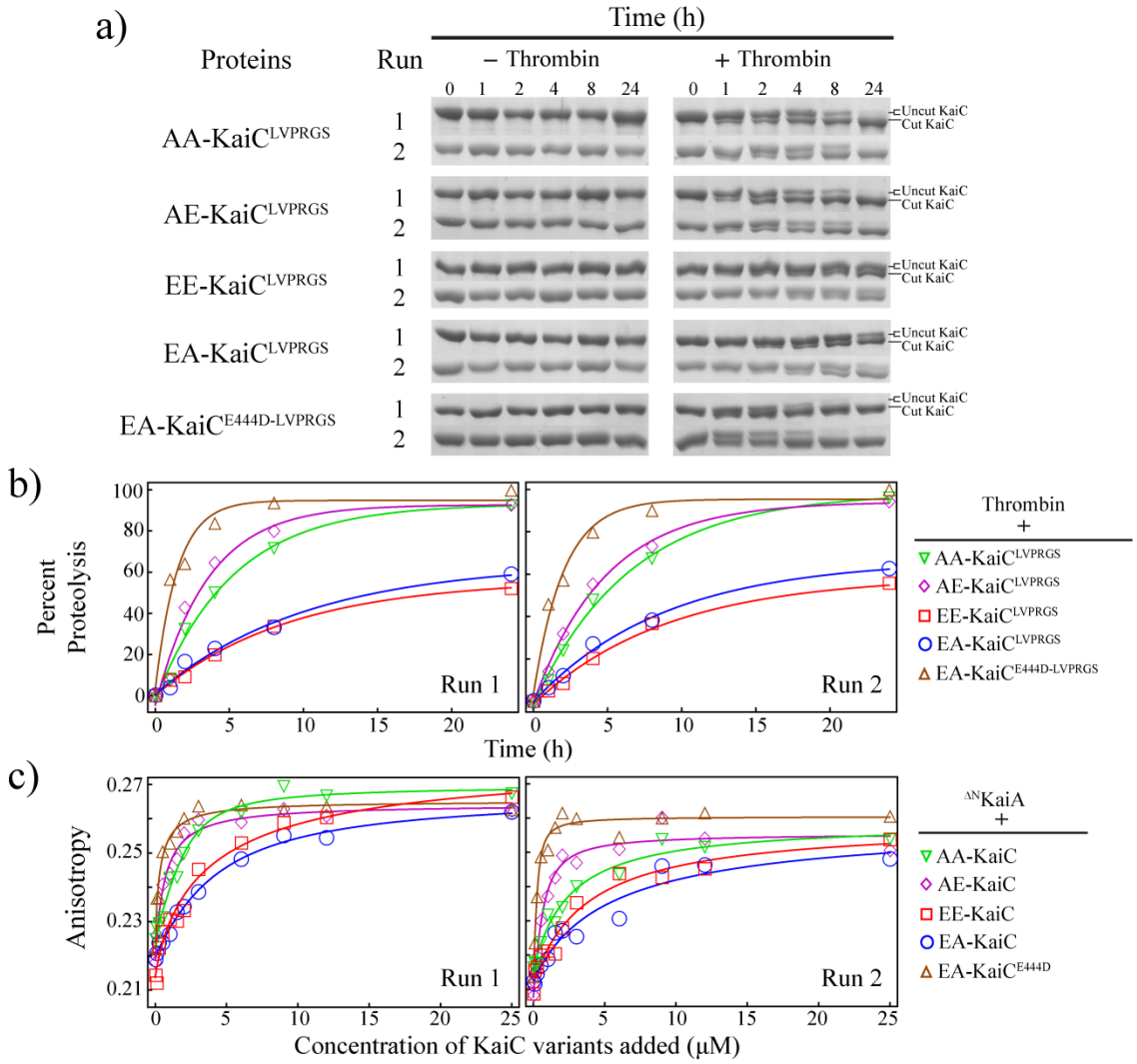

Fig. S6.

(a) A-loop proteolysis resolved by SDS/PAGE of five variants of KaiC (AA-KaiC, AE-KaiC, EE-KaiC, EA-KaiC, and EA-KaiC^{E444D}) with a thrombin cut site (LVPRGS) replacing residues I497 to K502. Twenty-four hour runs +/- thrombin were performed in duplicate. (b) Percent proteolysis determined by densitometry of the bands in (a). k_{obs} values were determined by fitting the data to equation (5) on page 21 of the Supplementary Material. (c) Fluorescence anisotropy measurements of 6-IAF labeled $^{\Delta N}$KaiA interacting with five variants of KaiC (AA-KaiC, green; AE-KaiC, purple; EE-KaiC, red; EA-KaiC, blue; EA-KaiC^{E444D}, brown). Duplicate runs were performed as shown. Apparent dissociation constants, K_D^{app}, for $^{\Delta N}$KaiA-KaiC complexes were determined by fitting to equation (1) on page 19 of the Supplementary Material. For details on the protein constructs and experimental setup, please see Table S1.

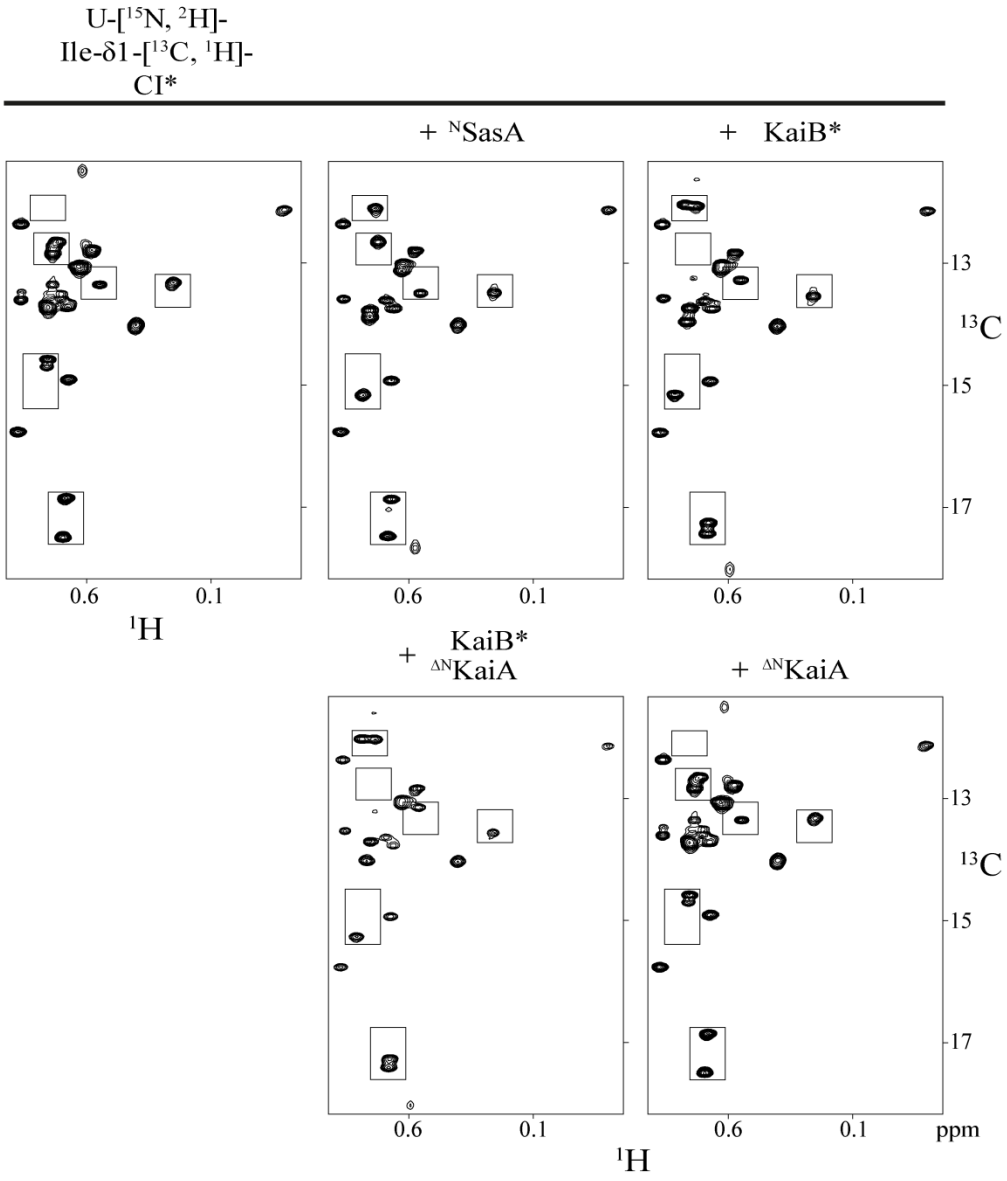

Fig. S7.

Methyl-TROSY spectra of U-[^{15}N, ^{2}H]-Ile-δ1-[^{13}C, ^{1}H]–labeled CI* alone (*top panel 1*), or in the presence of ^{N}SasA (*top panel 2*), KaiB* (*top panel 3*), KaiB* + $^{\Delta N}$KaiA (*bottom panel 1*), or $^{\Delta N}$KaiA (*bottom panel 2*). Boxed regions are shown in main text Fig. 7. All spectra were recorded with identical parameters, were processed identically and plotted at the same contour level. For details on the protein constructs and experimental setup, please see Table S1.

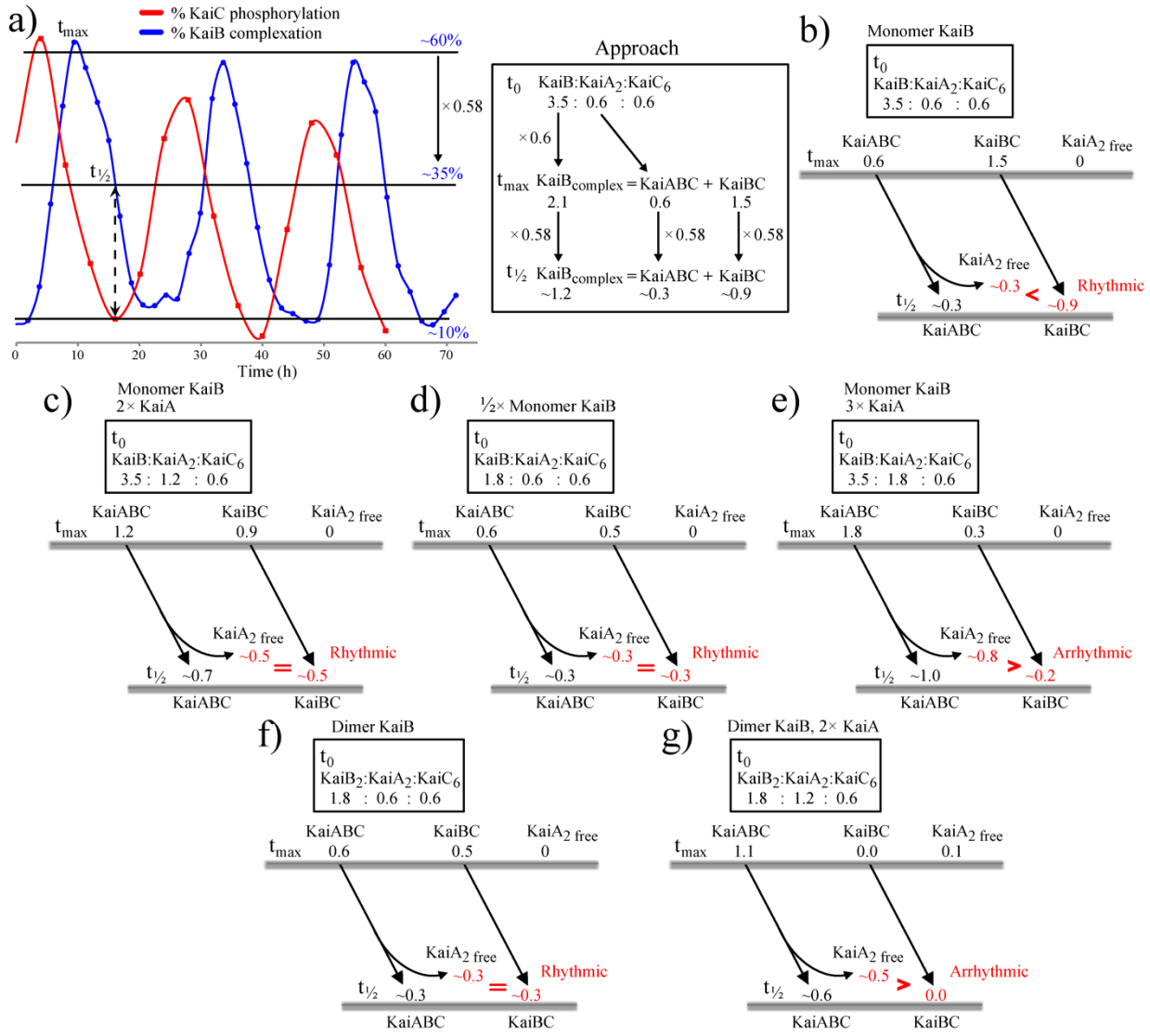

Fig. S8

Back-of-envelope calculations. (a) Adapted from Fig. 3d in Goda et al. 2012[1] (*left panel*). Red oscillation is percent KaiC phosphorylation, and blue oscillation is percent KaiB complexation (KaiBC and KaiABC). t_{max} marks the time of maximal complexation of KaiB, i.e., ~60% of total KaiB[1]. $t_{1/2}$ is the halfway point of disassociation of KaiB complexes, i.e., ~35% of total KaiB[1]. $t_{1/2}$ also corresponds to the lowest point of KaiC phosphorylation[1]. The goal is to estimate the level of desequestered KaiA [$KaiA_{2\ free}$] relative to that of [KaiBC] from $t_{max} \rightarrow t_{1/2}$, because (a) suggests that to be rhythmic desequestered KaiA needs to be resequestered during $t_{max} \rightarrow t_{1/2}$. Initial conditions are set at t_0. The box in (a) illustrates our approach, which is applied to panels (b) – (g). KaiB:$KaiA_2$:$KaiC_6$ at t_0 were taken from Nakajima et al. 2010[2] (see Table S2). Generally, $KaiB_{complex}$ at t_{max} equals t_0 KaiB × 0.6. $KaiB_{complex}$ at $t_{1/2}$ equals t_0 KaiB × 0.6 × 0.58. More specifically, we reason that at t_{max}, [$KaiABC(t_{max})$] = [$KaiA_2(t_0)$], and [$KaiBC(t_{max})$] = [$KaiB_{complex}(t_{max})$] – [$KaiABC(t_{max})$]. At $t_{1/2}$, [$KaiABC(t_{1/2})$] = [$KaiABC(t_{max})$] × 0.58 and [$KaiBC(t_{1/2})$] = [$KaiBC(t_{max})$] × 0.58. Likewise, [$KaiA_{2\ free}(t_{1/2})$] = [$KaiABC(t_{max})$] – [$KaiABC(t_{1/2})$]. In (b) – (e), we postulate a KaiB monomer sequesters a dimer of KaiA. In (f) and (g) we postulate that a KaiB dimer sequesters a dimer of KaiA.

Supplemental Tables

Table S1. Abbreviation and full name of *Thermosynechococcus elongatus* Kai proteins used in each experimental condition.

Experiment Type	[Abbreviation]-Protein Full Name (N-terminal Tag_Protein_Mutation_Length of Protein_ C-terminal Tag) / Final Concentration (μM)	Experimental Condition (all samples include 0.02% w/v ratio of NaN_3)
Analytical Gel Filtration Chromatography (Fig. 2, Fig. 6, Fig. S1a.)	1) [$^{\Delta N}$KaiA]-FLAG_KaiA_147-283 / 50, 100, 150 2) [KaiB*]-FLAG_KaiB_Y8A-Y94A_1-94_FLAG / 50 3) [CI*]-FLAG_CI-KaiC_R41A-K173A_1-247_FLAG / 50 4) [CI*$^{\Delta}$]-FLAG_CI-KaiC_R41A-K173A-Δ116-123_1-247_FLAG / 50 5) [^{N}SasA]-FLAG_SasA_P16A_16-107_FLAG / 50	• Volume: 250 μL • Pre-experiment incubation time of mixture: 4 hrs • Temperature: 30 °C • Buffer: 20 mM Tris, 50 mM NaCl, 5 mM DTT, 1 mM ATP, 1 mM $MgCl_2$, pH 7
Analytical Gel Filtration Chromatography (Fig. S1b.)	1) [EE-KaiC^{497}]-FLAG_KaiC_S431E-T432E_1-497_ / 50 2) [KaiB]-AMA_KaiB / 50	• Volume: 250 μL • Pre-experiment incubation time of mixture: 24 hrs • Temperature: 30 °C • Buffer: 20 mM Tris, 50 mM NaCl, 5 mM DTT, 1 mM ATP, 1 mM $MgCl_2$, pH 7
Fluorescence Spectroscopy (Fig. 3b)	1) [KaiB]-AMA_KaiB_A54C (6-IAF-labeled) / 0.02 2) [CI*]-FLAG_CI-KaiC_R41A-K173A_1-247_FLAG / 1, 5, 10, 20, 40, 150 3) KaiA / 5	• Volume: 300 μL • Pre-experiment incubation time of mixture: 24 hrs • Temperature: 25 °C • Buffer: 20 mM Tris, 50 mM NaCl, 5 mM DTT, 1 mM ATP, 1 mM $MgCl_2$, pH 7

Fluorescence Spectroscopy (Fig. S4a.)	1) [KaiB]-AMA_KaiB_A54C (6-IAF-labeled) / 0.02 2) [CI*]-FLAG_CI-KaiC_R41A-K173A_1-247_FLAG / 5 3) KaiA / 5	• Volume: 400 μL • Pre-experiment incubation time: 20 mins • Experiment time: 24 hrs • Temperature: 25 °C • Buffer: 20 mM Tris, 50 mM NaCl, 5 mM DTT, 1 mM ATP, 1 mM $MgCl_2$, pH 7 • Measurement time interval: every 30 mins
Fluorescence Spectroscopy (Fig. 4, Fig. S6c.)	1) [$^{\Delta N}$KaiA]-KaiA_147-283 (6-IAF-labeled) / 0.2 2) [AA-KaiC]-FLAG_KaiC_S431A-T432A / 0, 0.1, 0.25, 0.5, 1, 1.5, 2, 3, 6, 9, 12, 25 3) [AE-KaiC]-FLAG_KaiC_S431A-T432E / 0, 0.1, 0.25, 0.5, 1, 1.5, 2, 3, 6, 9, 12, 25 4) [EE-KaiC]-FLAG_KaiC_S431E-T432E / 0, 0.1, 0.25, 0.5, 1, 1.5, 2, 3, 6, 9, 12, 25 5) [EA-KaiC]-FLAG_KaiC_S431E-T432A / 0, 0.1, 0.25, 0.5, 1, 1.5, 2, 3, 6, 9, 12, 25 6) [EA-KaiC^{E444D}]-FLAG_KaiC_S431E-T432A-E444D / 0, 0.1, 0.25, 0.5, 1, 1.5, 2, 3, 6, 9, 12, 25	• Volume: 300 μL • Pre-experiment incubation time of mixture: 20 mins • Temperature: 25 °C • Buffer: 20 mM Tris, 50 mM NaCl, 5 mM DTT, 1 mM ATP, 1 mM $MgCl_2$, pH 7
Fluorescence Spectroscopy (Fig. 5a, Fig. S4b.)	1) [^{N}SasA]-FLAG_SasA_P16A-G57C_16-107_FLAG (6-IAF-labeled) / 0.025 2) [EE-KaiC^{497}]-FLAG_KaiC_S431E-T432E_1-497 / 2.5 3) [KaiB*]-FLAG_KaiB_Y8A-Y94A_1-94 / 10 4) [KaiB]-AMA_KaiB / 10 5) KaiA / 10, 20 6) [$^{\Delta N}$KaiA]-FLAG_KaiA_147-283 / 10, 20	• Volume: 400 μL • Pre-experiment incubation time: 2 hrs • Experiment time: 8 hrs • Temperature: 30 °C • Buffer: 20 mM Tris, 50 mM NaCl, 5 mM DTT, 1 mM ATP, 1 mM $MgCl_2$, pH 7 • Measurement time interval: 1.67, 2.5, 5 and 10 mins, then every 20 mins hereafter. (additional 0.2 and 0.41 mins were added for KaiB* measurement)

Fluorescence Spectroscopy (Fig. 5b, Fig. S4c.)	1) [^{N}SasA]-FLAG_SasA_P16A-G57C_16-107_FLAG (6-IAF-labeled) / 0.025 2) [CI*]-FLAG_CI-KaiC_R41A-K173A_1-247_FLAG / 2.5 3) [KaiB*]-FLAG_KaiB_Y8A-Y94A_1-94 / 10 4) [KaiB]-AMA_KaiB / 10 5) KaiA / 10, 20 6) [$^{\Delta N}$KaiA]-FLAG_KaiA_147-283 / 10, 20	• Volume: 400 µL • Pre-experiment incubation time: 20 mins • Experiment time: 24 hrs • Temperature: 30 °C • Buffer: 20 mM Tris, 50 mM NaCl, 5 mM DTT, 1 mM ATP, 1 mM $MgCl_2$, pH 7 • Measurement time interval: 2.5, 5, and 10 mins, then every 20 mins hereafter
In Vitro KaiC Phosphorylation Reactions (Fig. S3a-b)	1) KaiA / 1.67 2) [$^{\Delta N}$KaiA]-FLAG_KaiA_147-283 / 1.67 3) [KaiB]-AMA_KaiB / 5 4) [KaiC]-FLAG_KaiC / 5	• Volume: 200 µL • Experiment time: 24 hrs • Temperature: 35 °C • Buffer: 20 mM Tris, 150 mM NaCl, 0.5 mM EDTA, 1 mM ATP, 5 mM MgCl2, pH 7.0
Autodephosphorylation Reactions of KaiC and KaiC^{E444D} (Fig. S3c.)	1) [KaiC]-FLAG_KaiC / 10 2) [KaiC^{E444D}]-FLAG_KaiC_E444D / 10	• Volume: 50 µL • Experiment time: 24 hrs • Temperature: 37 °C • Buffer: 20 mM Tris, 150 mM NaCl, 0.5 mM EDTA, 1 mM ATP, 5 mM $MgCl_2$, pH 7.0
Autodephosphorylation Reactions of KaiC and KaiC^{E444D} with λ phosphatase (Fig. S3d.)	1) [KaiC]-FLAG_KaiC / 10 2) [KaiC^{E444D}]-FLAG_KaiC_E444D / 10	• Volume: 50 µL • Experiment time: 2 hrs • Temperature: 30°C • Buffer: 20 mM Tris, 50 mM NaCl, 1 mM ATP, 1 mM $MgCl_2$, 5mM $MnCl_2$, pH 7.0 • λ phosphatase added: 4000 units • λ phosphatase inhibitor added: 50 mM EDTA

A-loop Proteolysis (Fig. 4, Fig. S6a-b.)	1) [AA-KaiC^{LVPRGS}]-FLAG_KaiC_S431A-T432A-I497L-S498V-V499P-D500R-E501G-K502S / 10 2) [AE-KaiC^{LVPRGS}]-FLAG_KaiC_S431A-T432E-I497L-S498V-V499P-D500R-E501G-K502S / 10 3) [EE-KaiC^{LVPRGS}]-FLAG_KaiC_S431E-T432E-I497L-S498V-V499P-D500R-E501G-K502S / 10 4) [EA-KaiC^{LVPRGS}]-FLAG_KaiC_S431E-T432A-I497L-S498V-V499P-D500R-E501G-K502S / 10 5) [EA-KaiC$^{E444D\text{-}LVPRGS}$]-FLAG_KaiC_S431E-T432A-E444D-I497L-S498V-V499P-D500R-E501G-K502S /10	• Volume: 100 µL • Experiment time: 24 hrs • Temperature: 30 °C • Buffer: 20 mM Tris, 50 mM NaCl, 1 mM ATP, 1 mM $MgCl_2$, pH 7 • Thrombin added: 2 units
NMR Methyl-TROSY (Fig. 3a, Fig. S2.)	1) [$^{\Delta N}$KaiA]-FLAG_KaiA_147-283 (U-[^{15}N, ^{2}H]-Ile-1-[^{13}C, ^{1}H] labeled) / 20 2) [KaiB*]-FLAG_KaiB_Y8A-Y94A_1-94 / 50, 100, 200 3) [KaiB]-AMA_KaiB / 50, 200 4) [CI*]-FLAG_CI-KaiC_R41A-K173A_1-247_FLAG / 50 5) [CII*]-FLAG_CII-KaiC_S431E-T432E-E444D_249-518 / 50	• Volume: 350 µL • Pre-experiment incubation time of mixture: 8 hrs • Number of scan: 256 • ^{1}H / ^{13}C sweep width (ppm): 6.48 / 8.00 • ^{1}H / ^{13}C carrier (ppm): -0.657 / 13.397 • ^{1}H / ^{13}C acquisition time (ms): 64.0 / 82.7 • Temperature: 30 °C • Buffer in 99.96 % D_2O: 20 mM Tris, 75 mM NaCl, 5 mM DTT, 1 mM ATP, 1 mM $MgCl_2$, 10 µM DSS, pH 7 • Shaped tube

NMR Methyl-TROSY (Fig.7, Fig. S7.)	1) [CI*]-FLAG_CI-KaiC_R41A-K173A_1-247_FLAG (U-[^{15}N, ^{2}H]-Ile-1-[^{13}C, ^{1}H] labeled) / 20 2) [^{N}SasA]-FLAG_SasA_P16A_16-107_FLAG / 50 3) [KaiB*]-FLAG_KaiB_Y8A-Y94A_1-94 / 50 4) [$^{\Delta N}$KaiA]-FLAG_KaiA_147-283 / 50	• Volume: 350 μL • Number of scan: 256 • ^{1}H / ^{13}C sweep width (ppm): 6.48 / 8.00 • ^{1}H / ^{13}C carrier (ppm): -0.609 / 13.445 • ^{1}H / ^{13}C acquisition time (ms): 64.0 / 82.7 • Temperature: 30 °C • Buffer in 99.96 % D_2O: 20 mM Tris, 50 mM NaCl, 5 mM DTT, 1 mM ATP, 1 mM $MgCl_2$, 10 μM DSS, pH 7 • Shaped tube
NMR ^{15}N-TROSY (Fig. S5a.)	1) [KaiB*]-FLAG_KaiB_Y8A-Y94A_1-94 (U-[^{15}N, ^{2}H] labeled) / 150 2) [$^{\Delta N}$KaiA]-FLAG_KaiA_147-283 / 675	• Volume: 350 μL • Pre-experiment incubation time of mixture: 8 hrs • Number of scan: 128 (free KaiB*), 256 (KaiB* + $^{\Delta N}$KaiA) • ^{1}H / ^{15}N sweep width (ppm): 16.00 / 26.48 • ^{1}H / ^{15}N carrier (ppm): 4.696 / 119.279 • ^{1}H / ^{15}N acquisition time (ms): 69.8 / 79.4 • Temperature: 30 °C • Buffer in 5% D_2O: 5 mM Tris, 50 mM NaCl, 10 μM DSS, pH 7 • Shaped tube

NMR ^{15}N-TROSY (Fig. S5b.)	1) [CI*]-FLAG_CI-KaiC_R41A-K173A_1-247_FLAG (U-[^{15}N] labeled) / 50 2) [CI*$^{\Delta}$]-FLAG_CI-KaiC_R41A-K173A-Δ116-123_1-247_FLAG (U-[^{15}N] labeled) / 50	• Volume: 350 μL • Number of scan: 512 • ^{1}H / ^{15}N sweep width (ppm): 18.00 / 35.23 • ^{1}H / ^{15}N carrier (ppm): 4.756 / 119.628 • ^{1}H / ^{15}N acquisition time (ms): 64.9 / 29.8 • Temperature: 25 °C • Buffer in 5% D_2O: 20 mM Tris, 50 mM NaCl, 5 mM DTT, 1 mM ADP, 1 mM $MgCl_2$, 10 μM DSS, pH 7 • Shaped tube
NMR ^{15}N-TROSY (Fig. S5c.)	1) [^{N}SasA]-FLAG_SasA_P16A_16-107 (U-[^{15}N] labeled) / 80 2) [CI*]-FLAG_CI-KaiC_R41A-K173A_1-247_FLAG / 156	• Volume: 350 μL • Number of scan: 264 • ^{1}H / ^{15}N sweep width (ppm): 16.00 / 26.48 • ^{1}H / ^{15}N carrier (ppm): 4.746 / 119.331 • ^{1}H / ^{15}N acquisition time (ms): 69.8 / 79.4 • Temperature: 25 °C • Buffer in 5% D_2O: 20 mM Tris, 50 mM NaCl, 10 μM DSS, pH 7 • Shaped tube

Table S2. Back-of-envelope calculation of KaiA-KaiB complex stoichiometry compared with published experimental results.

Original experimental setup from Nakajima et al. 2010[2] (μM monomer concentration).	KaiB:KaiA:KaiC 3.5 : 1.2 : 3.5	KaiB:KaiA:KaiC 3.5 : 2.4 : 3.5	KaiB:KaiA:KaiC 1.8 : 1.2 : 3.5	KaiB:KaiA:KaiC 3.5 : 3.6 : 3.5
Nakajima et al. 2010[2] setup converted to dimer KaiA and hexamer KaiC (μM concentration).	KaiB:$KaiA_2$:$KaiC_6$ 3.5 : 0.6 : 0.6	KaiB:$KaiA_2$:$KaiC_6$ 3.5 : 1.2 : 0.6	KaiB:$KaiA_2$:$KaiC_6$ 1.8 : 0.6 : 0.6	KaiB:$KaiA_2$:$KaiC_6$ 3.5 : 1.8 : 0.6
Experimental result from Nakajima et al. 2010[2].	Rhythmic	Rhythmic	Rhythmic	Arrhythmic
Assuming a monomer of KaiB sequesters a dimer of KaiA.	Rhythmic, Fig. S8b	Rhythmic, Fig. S8c	Rhythmic, Fig. S8d	Arrhythmic, Fig. S8e
Assuming a dimer KaiB sequesters a dimer of KaiA.	Rhythmic, Fig. S8f	Arrhythmic, Fig. S8g	Arrhythmic, not shown	Arrhythmic, not shown

Materials and Methods

Analytical Gel Filtration Chromatography

Binding of $^{\Delta N}$KaiA with KaiB* and/or CI*

The samples assayed included: $^{\Delta N}$KaiA alone (50 μM), KaiB* alone (50 μM), CI* alone (50 μM), $^{\Delta N}$KaiA (50 μM) + KaiB* (50 μM), $^{\Delta N}$KaiA (50 μM) + CI* (50 μM), CI* (50 μM) + KaiB* (50 μM), $^{\Delta N}$KaiA (50 μM) + CI* (50 μM) + KaiB* (50 μM), 2× $^{\Delta N}$KaiA (100 μM) + CI* (50 μM) + KaiB* (50 μM), and 3× $^{\Delta N}$KaiA (150 μM) + CI* (50 μM) + KaiB* (50 μM). Each sample was incubated in the binding buffer (20 mM Tris, 50 mM NaCl, 1 mM ATP, 1 mM $MgCl_2$, 5 mM DTT, 0.02% NaN_3, pH 7.0) at 30°C for 4 hours and then applied to a Superdex 200 10/300 GL column with a flow rate of 0.5 mL/min, at room temperature. The volume of the sample loop was 100 μL. For details on the protein constructs and experimental setup, please see Table S1.

Binding of ^{N}SasA or KaiB* with CI* or CI*$^{\Delta}$

The samples assayed included: CI* alone (50 μM), CI*$^{\Delta}$ alone (50 μM), KaiB* alone (50 μM), ^{N}SasA alone (50 μM), CI* (50 μM) + KaiB* (50 μM), CI*$^{\Delta}$ (50 μM) + KaiB* (50 μM). CI* (50 μM) + ^{N}SasA (50 μM), and CI*$^{\Delta}$ (50 μM) + ^{N}SasA (50 μM). Each sample was incubated in the binding buffer (20 mM Tris, 50 mM NaCl, 1 mM ATP, 1 mM $MgCl_2$, 5 mM DTT, 0.02% NaN_3, pH 7.0) at 30°C for 4 hours and then applied to a Superdex 200 10/300 GL column with a flow rate of 0.5 mL/min, at room temperature. The volume of the sample loop was 100 μL. For details on the protein constructs and experimental setup, please see Table S1.

Molecular weight markers used to calibrate the size-exclusion columns

Ferritin (440 kDa), albumin (67 kDa), ovalbumin (43 kDa), and ribonuclease A (13.7 kDa) from the gel-filtration HMW and LMW calibration kits (GE Healthcare) were used as molecular weight markers.

Fluorescence Spectroscopy

Photon Counting Spectrofluorimeter Set-up

A ISS PC1 spectrofluorimeter was operated by using the Vinci software provided. A water bath (VWR International) was connected to the spectrofluorimeter to control the temperature of the cuvette compartment. Excitation wavelength and slit width were 492 nm and 2 mm, respectively, with a 497/16 nm BrightLine® single-band bandpass filter installed. Emission wavelength and slit width were 530 nm and 2 mm, respectively, with a 524/24 nm BrightLine® single-band bandpass filter and monochromator installed. Detailed setup was followed as previously described[3].

Dependence of fluorescence anisotropy of 6-IAF-labeled $^{\Delta N}$KaiA on concentrations of five KaiC variants (AA-KaiC, AE-KaiC, EE-KaiC, EA-KaiC, EA-KaiC^{E444D}) to determine K_D^{app} values

0.2 μM samples of 6-IAF-labeled $^{\Delta N}$KaiA were titrated with 0.1, 0.25, 0.5, 1, 1.5, 2, 3, 6, 9, 12 and 25 μM of each KaiC variant (AA-KaiC, AE-KaiC, EE-KaiC, EA-KaiC, EA-KaiC^{E444D}) at 25°C in a reaction buffer (20 mM Tris, 50 mM NaCl, 5 mM DTT, 1 mM ATP ,1 mM $MgCl_2$, pH 7.0). Each sample was incubated at 25°C for 20 minutes to reach thermal equilibrium before anisotropy experiments. Five measurements were taken at each KaiC concentration and their average anisotropy was used for plotting. Because of the relative concentrations of $^{\Delta N}$KaiA and KaiC[4], data were fit to equation (1) using Mathematica,

$$F = Fmin + (Fmax - Fmin)\ \frac{[L]+[P]+KDapp-\sqrt{([L]+[P]+KDapp)^2-4[L][P]}}{2[P]} \qquad (1)$$

where F is fluorescence anisotropy, $[P]$ is total concentration of fluorophore-labeled protein, and $[L]$ is total concentration of ligand added. The standard errors were estimated from duplicate runs. For details on the protein constructs and experimental setup, please see Table S1.

Fluorescence anisotropy derived K_D^{app} values for 6-IAF-labeled KaiB + CI* ± KaiA

0.02 μM samples of 6-IAF-labeled KaiB were titrated with 1, 5, 10, 20, 40 and 150 μM of CI* at 25°C in a reaction buffer (20 mM Tris, 50 mM NaCl, 5 mM DTT, 1 mM ATP ,1 mM $MgCl_2$, pH 7.0) ± 5 μM KaiA. Each sample was incubated at 25°C for 24 hours to reach thermal equilibrium before anisotropy measurements. Five measurements were taken for each sample and their average anisotropy was used for plotting. Because the total ligand concentration approximated free ligand concentration in this experimental setup[4], the values of K_D^{app} were fit to equation (2) using Mathematica,

$$F = Fmin + (Fmax - Fmin)\ \frac{[L]}{[L]+KDapp} \qquad (2)$$

where F is fluorescence anisotropy, $[L]$ is total concentration of ligand added. The standard error was estimated from duplicate runs. For details on the protein constructs and experimental setup, please see Table S1.

Binding kinetics of 6-IAF-labeled KaiB with CI* ± KaiA determined by fluorescence anisotropy experiments

0.02 μM samples of 6-IAF-labeled KaiB were mixed with 5 μM of CI* at 25°C in a reaction buffer (20 mM Tris, 50 mM NaCl, 5 mM DTT, 1 mM ATP ,1 mM $MgCl_2$, pH 7.0) ± 5 μM KaiA. The labeled protein and titrate were incubated separately at 25°C for 20 minutes to reach 25°C before mixing. The kinetic anisotropy measurements started immediately after addition of the titrate with a dead time of ~5s. One measurement was taken for each time point for the course of 24 hours. Association curves were fit to equation (3) using Mathematica,

$$F = (Fmax - Fmin)(1 - e^{-kobst}) + Fmin \qquad (3)$$

where F is fluorescence anisotropy, and t is in hours. For details on the protein constructs and experimental setup, please see Table S1.

Binding kinetics of 6-IAF-labeled ^{N}SasA to EE-KaiC^{497} in competition with KaiB or KaiB* ± KaiA or $^{\Delta N}$KaiA, by fluorescence anisotropy

0.025 μM of 6-IAF-labeled ^{N}SasA and 2.5 μM EE-KaiC^{497} were incubated at 30°C in a reaction buffer (20 mM Tris, 50 mM NaCl, 5 mM DTT, 1 mM ATP ,1 mM $MgCl_2$, pH 7.0) for 2 hours before adding: KaiB* (10 μM), KaiB (10 μM), KaiB (10 μM) + KaiA (10 μM), KaiB (10 μM) + KaiA (20 μM), KaiB (10 μM) + $^{\Delta N}$KaiA (10 μM), KaiB (10 μM) + $^{\Delta N}$KaiA (20 μM), KaiA (20 μM), and $^{\Delta N}$KaiA (20 μM). The kinetic anisotropy measurements started immediately after mixing proteins with a dead time of ~5s. One measurement was taken for each time point for the course of 24 hours. Data were fit to equation (4) using Mathematica,

$$F = (Fmax - Fmin)(e^{-kobst}) + Fmin \qquad (4)$$

where F is fluorescence anisotropy, and t is in hours. For details on the protein constructs and experimental setup, please see Table S1.

Binding kinetics of 6-IAF-labeled ^{N}SasA to CI* in competition with KaiB or KaiB* ± KaiA or $^{\Delta N}$KaiA, by fluorescence anisotropy

0.025 μM of 6-IAF-labeled ^{N}SasA and 2.5 μM CI* were incubated in 30°C in a reaction buffer (20 mM Tris, 50 mM NaCl, 5 mM DTT, 1 mM ATP ,1 mM $MgCl_2$, pH 7.0) for 20 minutes before adding: KaiB* (10 μM), KaiB (10 μM), KaiB (10 μM) + KaiA (10 μM), KaiB (10 μM) + KaiA (20 μM), KaiB (10 μM) + $^{\Delta N}$KaiA (10 μM), KaiB (10 μM) + $^{\Delta N}$KaiA (20 μM), KaiA (20 μM) and $^{\Delta N}$KaiA (20 μM). The kinetic anisotropy measurement started immediately after addition of the titrate with a dead time of ~5s. One iteration was taken for each time point for the course of 24 hours. Data were fit to equation (4) using Mathematica. Details on the protein constructs and experimental setup are provided in Table S1.

In Vitro KaiC Phosphorylation Reactions

KaiC was preincubated at 37°C for 24 hours to allow samples to autodephosphorylate to low levels of phosphorylation before use in experiments. KaiC proteins were then incubated with KaiB and KaiA (or $^{\Delta N}$KaiA), in a reaction buffer (20 mM Tris, 150 mM NaCl, 0.5 mM EDTA, 1 mM ATP, 5 mM $MgCl_2$, 0.02% NaN_3, pH 7.0) at 35°C. The final concentrations of KaiA (or $^{\Delta N}$KaiA), KaiB, and KaiC were 1.67, 5, and 5 μM, respectively. 10 μL aliquots were taken at indicated time points from the reaction mixtures for SDS-PAGE analysis. The reaction of each time point was stopped by adding 10 μL of SDS-PAGE gel-loading dye (100 mM Tris, 4% SDS, 0.2% bromophenol blue, 20% glycerol, 400 mM β-mercaptoethanol, pH 6.8) and freezing at -20°C. Details of the running conditions for SDS-PAGE and densitometric analysis have been described previously[3]. Details on the protein constructs and experimental setup are provided in Table S1.

Autodephosphorylation Reactions of KaiC and KaiC^{E444D} ± λ phosphatase

<u>Without λ phosphatase</u>

10 μM of KaiC and KaiC^{E444D} were incubated at 37°C for 24 hours in a reaction buffer (20 mM Tris, 150 mM NaCl, 0.5 mM EDTA, 1 mM ATP, 5 mM $MgCl_2$, 0.02% NaN_3, pH 7.0). 10 μL aliquots were taken at indicated time points from the reaction mixtures for SDS-PAGE analysis. The reaction of each time point was stopped by adding 10 μL of SDS-PAGE gel-loading dye (100 mM Tris, 4% SDS, 0.2% bromophenol blue, 20% glycerol, 400 mM β-mercaptoethanol, pH 6.8) and freezing at -20°C. Details of the running conditions for SDS-PAGE and densitometric analysis were the same as for in vitro KaiC phosphorylation reactions. Details on the protein constructs and experimental setup are provided in Table S1.

With λ phosphatase

10 μM of KaiC and KaiC^{E444D} were incubated at 30°C for 2 hours in a reaction buffer (20 mM Tris, 50 mM NaCl, 1 mM ATP, 1 mM $MgCl_2$, 5mM $MnCl_2$, 0.02% NaN_3, pH 7.0) with 4000 units of λ phosphatase (New England BioLabs Inc.) ± 50 mM EDTA (λ phosphatase inhibitor). As a control, buffer was added instead of λ phosphatase. 10 μL aliquots were taken at indicated time points from the reaction mixtures for SDS-PAGE analysis. The reaction of each time point was stopped by adding 10 μL of SDS-PAGE gel-loading dye (100 mM Tris, 4% SDS, 0.2% bromophenol blue, 20% glycerol, 400 mM β-mercaptoethanol, pH 6.8) and freezing at -20°C. Details of the running conditions for SDS-PAGE and densitometric analysis were the same as for in vitro KaiC phosphorylation reactions. Details on the protein constructs and experimental setup are provided in Table S1.

Kinetics of A-loop Proteolysis

Proteolysis experiments were carried out using 10 μM of each of the five KaiC variants (AA-KaiC, AE-KaiC, EE-KaiC, EA-KaiC, and EA-KaiC^{E444D}) with a thrombin cut site (LVPRGS) replacing residues I497 to K502. KaiC samples were mixed with 2 units of thrombin (Sigma) and incubated at 30°C in a reaction buffer (20 mM Tris, 50 mM NaCl, 1 mM ATP, 1 mM $MgCl_2$, 0.02% NaN_3, pH 7.0). For control experiments, buffer was added instead of thrombin. 10 μL aliquots were taken at indicated time points in Fig. S6 from the reaction mixtures for SDS-PAGE analysis. The reaction of each time point was stopped by adding of 10 μL of SDS-PAGE gel-loading dye (100 mM Tris, 4% SDS, 0.2% bromophenol blue, 20% glycerol, 400 mM β-mercaptoethanol, pH 6.8) and freezing at -20°C. The samples were loaded onto gels: 9 x 10 cm SDS polyacrylamide gels (4% of acrylamide/bisacrylamide for stacking gel, and 9% of acrylamide/bisacrylamide for running gel) with 15 wells (10 x 3 x 0.75 mm). The gels were subjected to electrophoresis at 60 volts in glycine buffer for 30 minutes and then at 140 volts for 120 minutes, with the buffer chamber surrounded by ice. Gels were stained with Coomassie brilliant blue R250. The percentage of thrombin proteolysis product in each lane was determined by densitometric analysis using Image J (National Institutes of Health) and PeakFit (SeaSolve Software, Inc.). The k_{obs} values were fit to equation (5) using Mathematica,

$$P(t) = (Pmax - Pmin)(1 - e^{-kobst}) + Pmin \qquad (5)$$

where $P(t)$ is percentage of cut product at time t (hours). *Pmin* and *Pmax* are respectively the percent cut at $t = 0$, and $t = \infty$. The standard error was estimated from duplicate runs. For details on the protein constructs and experimental setup, please see Table S1.

NMR Spectroscopy

All NMR experiments were run on a Bruker 600MHz AVANCE III spectrometer equipped with a TCI cryoprobe. Chemical shifts were referenced to internal DSS. Data were processed using NMRPipe and visualized using NMRDraw[5]. For details on the protein constructs and experimental setup, please see Table S1.

Cloning and Constructs of *kaiA*, *kaiB*, and *kaiC*

All genes were cloned into pET-28b using the Nde I/Hind III sites by PCR. The gene encoding SUMO was spliced with the *kai* genes using PCR. Details of the cloning protocol have been described previously[3]. Please see Table S1 for the list of protein constructs.

Protein Expression, Purification, and Fluorescence Labeling

Overview

The pET-28b plasmids harboring *kaiA, kaiB,* or *kaiC* were used to transform *Escherichia coli* BL21(DE3) cells (Novagen). Cells were grown in LB (H_2O), M9 (H_2O), and M9 (D_2O) media for production of unlabeled, U-[^{15}N, ^{1}H]-labeled, and [^{15}N, ^{2}H, $^{1}H^{N}$]-labeled or U-[^{15}N, ^{2}H]-Ile-δ1-[^{13}C, ^{1}H]-labeled proteins, respectively. IPTG (isopropyl β-D-1-thiogalactopyranoside) (Research Products International) at a final concentration of 0.2 mM was added to induce protein expression when OD_{600} reached 0.4-0.6. The induction time was ~12 h at 25°C for over-expression of unlabeled proteins, or ~12 h for production of ^{15}N-labeled, or [^{15}N, ^{2}H, $^{1}H^{N}$]-labeled or U-[^{15}N, ^{2}H]-Ile-δ1-[^{13}C, ^{1}H]-labeled proteins. Cells were harvested by centrifugation at 5,000 rpm for 15 min, followed by cell lysis and protein purification. Proteins were purified by Ni-NTA affinity chromatography and gel filtration chromatography. The disposable 10 ml Polypropylene Columns (Thermo Scientific) packed with Ni-NTA agarose (VWR) were used for Ni-NTA gravity chromatography, whereas pre-packed columns including HiLoad 16/60 Superdex 75 Column (GE Healthcare), and HiLoad 16/60 Superdex 200 Column (GE Healthcare) were used for gel-filtration chromatography.

Labeling proteins with 6-IAF (Invitrogen) was achieved by adding the dye to protein samples at a 5:1 dye:protein molar ratio followed by overnight incubation of the mixture at 4°C in darkness. A subsequent desalting step was applied to remove residual dye. Note that the protein samples were supplemented with 1 mM TCEP before addition of the dye to keep the Cys residues reduced for efficient fluorescence labeling. All protein samples were concentrated with Amicon Stirred Ultrafiltration Cell (Millipore) by applying nitrogen gas at 45 psi and using a YM-10 ultrafiltration membrane (Millipore). Protein concentrations were determined using Coomassie Plus Assay (Pierce) by following the manufacturer's protocol. The absorbance for BSA at a series of concentrations (0, 0.2, 0.4, 0.6, and 0.8 mg/ml) was obtained to generate the standard curve. The protein (or BSA) and dye volumes were 5 μL and 150 μL, respectively. The volume for OD_{595} measurement was 100 μL. The OD_{595} reading was obtained on a DU 640 UV/VIS spectrophotometer (Beckman).

Expression of unlabeled proteins

The protocol has been described previously[3].

Expression of U-[^{15}N, ^{1}H]-labeled proteins using M9 (H_2O) minimal medium

The protocol has been described previously[3].

Expression of unlabeled proteins using M9 (H_2O) minimal medium

Only KaiC, KaiC^{497} and KaiC phosphomimic variants (±vthrombin cut site) were expressed in this medium for higher yield and purity. The detailed protocol is the same as for expression of ^{15}N-labeled proteins, except $^{14}NH_4Cl$ was used instead of $^{15}NH_4Cl$.

Expression of U-[^{15}N, ^{2}H]-Ile-δ1-[^{13}C,^{1}H]-labeled proteins

The protocol has been described previously[3].

Expression of [^{15}N, ^{2}H, $^{1}H^{N}$]-labeled proteins

The protocol has been described previously[3].

Purification of Ulp1, KaiA, KaiB, and KaiC.

The protocol has been described previously[3].

Reference

1. Goda K., Ito H., Kondo T. & Oyama T. (2012) Fluorescence Correlation Spectroscopy to Monitor Kai Protein-based Circadian Oscillations in Real Time. *Journal of Biological Chemistry* **287,** 3241-3248. 10.1074/jbc.M111.265777.

2. Nakajima M., Ito H. & Kondo T. (2010) In vitro regulation of circadian phosphorylation rhythm of cyanobacterial clock protein KaiC by KaiA and KaiB. *FEBS Lett.* **584,** 898-902. 10.1016/j.febslet.2010.01.016.

3. Chang Y., Kuo N., Tseng R. & LiWang A. (2011) Flexibility of the C-terminal, or CII, ring of KaiC governs the rhythm of the circadian clock of cyanobacteria. *Proceedings of the National Academy of Sciences* **108,** 14431-14436. 10.1073/pnas.1104221108.

4. Pollard T. D. (2010) A Guide to Simple and Informative Binding Assays. *Molecular Biology of the Cell* **21,** 4061-4067. 10.1091/mbc.E10-08-0683.

5. Delaglio F., Grzesiek S., Vuister G. W., Zhu G., Pfeifer J. & Bax A. (1995) NMRPipe: A Multidimensional Spectral Processing System Based on UNIX Pipes. *J. Biomol. NMR* 6, 277-293.